STREAMLINE-BASED SIMULATION OF WATER INJECTION IN NATURALLY FRACTURED RESERVOIRS

A Thesis

by

AHMED AL-HUTHALI

Submitted to the Office of Graduate Studies of
Texas A&M University
in partial fulfillment of the requirements for the degree of

MASTER OF SCIENCE

August 2003

Major Subject: Petroleum Engineering

STREAMLINE-BASED SIMULATION OF WATER INJECTION IN NATURALLY FRACTURED RESERVOIRS

A Thesis

by

AHMED AL-HUTHALI

Submitted to the Office of Graduate Studies of
Texas A&M University
in partial fulfillment of the requirements for the degree of

MASTER OF SCIENCE

Approved as to style and content by:

Akhil Datta-Gupta (Chair of Committee)	W. John Lee (Member)
Richard L. Gibson (Member)	Hans C. Juvkam-Wold (Head of Department)

August 2003

Major Subject: Petroleum Engineering

ABSTRACT

Streamline Simulation of Water Injection in Naturally Fractured Reservoirs.

(August 2003)

Ahmed Al-Huthali, B.E., King Fahd University of Petroleum and Minerals

Chair of Advisory Committee: Dr. Akhil Datta-Gupta

The current streamline formulation is limited to single-porosity systems and is then not suitable for application to naturally fractured reservoirs. Describing the fluid transport in naturally fractured reservoirs has been recognized as a main challenge for simulation engineers due to the complicated physics involved.

In this work, we generalized the streamline-based simulation to describe the fluid transport in naturally fractured reservoirs. We implemented three types of transfer function: the conventional transfer function (CTF), the diffusion transfer function (DTF), and the empirical transfer function (ETF). We showed that these transfer functions can be implemented easily in the current single-porosity streamline codes. These transfer functions have been added as a source term to the transport equation that describes the saturation evolution along the streamlines. We solved this equation numerically for all types of transfer functions. The numerical solution of the continuity equation with DTF and ETF requires discretizing a convolution term. We derived an analytical solution to the saturation equation with ETF in terms of streamline TOF to validate the numerical solution. We obtain an excellent match between the numerical and the analytical solution.

The final stage of our study was to validate our work by comparing our dual-porosity streamline simulator (DPSS) to the commercial dual-porosity simulator, ECLIPSE. The dual-porosity ECLIPSE uses the CTF to describe the interaction between the matrix-blocks and the fracture system. The dual-porosity streamline simulator with CTF showed an excellent match with the dual-porosity ECLIPSE. On the other hand, dual-porosity

streamline simulation with DTF and ETF showed a lower recovery than the recovery obtained from the dual-porosity ECLIPSE and the DPSS with CTF. This difference in oil recovery is not due to our formulation, but is related to the theoretical basis on which CTF, DTF, and ETF were derived in the literature. It was beyond the scope of this study to investigate the relative accuracy of each transfer function.

We demonstrate that the DPSS is computationally efficient and ideal for large-scale field application. Also, we showed that the DPSS minimizes numerical smearing and grid orientation effects compared to the dual-porosity ECLIPSE.

DEDICATION

This thesis is dedicated to:

My parents for their love, support, sacrifices, and prayers;

My adorable wife, Lama, for her enduring patience, support, and prayers;

My father and mother in law for their support and prayers;

My upcoming child who hasn't seen the light yet.

ACKNOWLEDGMENTS

Praise and thanks to Almighty, The Most Merciful, who gave me the potential and the knowledge to accomplish this difficult task.

I would like to express my deepest appreciation to the chairman of the advisory committee, Dr. Akhil Datta-Gupta, for his invaluable supervision and support to complete this research. Sincere appreciation is extended to Dr. W. John Lee and Dr. Richard L. Gibson for serving as members on the advisory committee. Acknowledgements are due to Dr. Erwinsyah Putra for his useful discussions.

Further, I would like to thank my sponsor company, Saudi Aramco, for giving me the opportunity to pursue my master's degree.

The heaviest burden involved in accomplishing my study was borne by my wife. For her constant encouragement, support and enduring patience throughout the study, I owe her my hearty gratitude. Thanks are due to all members of the Saudi House who made my stay in College Station enjoyable.

Finally, it was a great pleasure to work with the reservoir characterization group at Texas A&M University.

TABLE OF CONTENTS

Page

LIST OF TABLES

Page

LIST OF FIGURES

Page

Page

Page

CHAPTER I
INTRODUCTION

This chapter describes the advantages and the applications of single-porosity streamline simulation. It presents a literature review summarizing the various works done in modeling fluid transport using single-porosity streamline simulation. Also, it provides a literature review on modeling the fluid transfer between matrix-blocks and fracture system. Moreover, this chapter discusses the motivations and the objectives of this study and states the methodology of achieving those objectives. Finally, it outlines the organization of this thesis.

1.1 Background

Although streamline technology has been around in the petroleum industry for several decades, its rapid development has been noticed only in the recent years. This rapid development was driven by the recent development in reservoir characterization. The current reservoir characterization technologies can generate large multi-million cell static-models. Simulating the fluid flow in these models using the conventional finite difference simulation is highly expensive and requires an extensive time. This has resulted in a steadily increased gap between flow simulation and static models. The 3D streamline-Based simulation is a promising technology which offers significant potential to reduce this gap and meet some of the simulation challenges.

Streamline-based simulation is highly efficient in solving large, geologically complex systems, where fluid flow is controlled by well positions and heterogeneity[1,2,3]. Streamline simulation has been applied successfully in wide range of petroleum engineering areas such as ranking geological models[4,5], 'upscaling' from fine-scale

---

This thesis follows the style and format of the *SPE Journal*.

models[4,5], injection efficiency[4] , well- allocation factors and pore volumes[4] , integration of water-cut and tracer data into reservoir description[6] , and history matching[4,6].

The streamline approach has the advantage of minimizing the numerical dispersion and grid orientation effects. Also, it offers efficient use of memory and high computational speed.

So far the application of streamline simulation has been limited to single-porosity system where the matrix provides the main path and storage for fluid. Nobody so far has reported how to model dual-porosity system using the streamline technique. In dual-porosity systems fractures provide the main path for flow while the matrix provides the main storage for fluid. Fractures and matrix are related by a transfer function that governs the exchange of fluid between the two media. Through this exchange of fluids, oil will be recovered from the matrix-blocks.

1.2 Literature Survey and Present Status

1.2.1 Streamline-Based Simulation in Single-Porosity System

Muskat[7] introduced an early definition to the governing analytical equations which describe the stream and potential functions in a homogenous 2D system for incompressible flow. Fay & Prats[8] and LeBlanc & Caudle[9] developed a numerical model for these functions to predict tracer and two-phase flow on a two-well homogenous 2D system.

Higgins and Leighton[10] introduced the idea of using the concept of streamtubes to predict the multi-phase displacements in porous media. They treated each streamtube as a one-dimensional system and used the Buckley-Leverett solution to map saturation along the streamtube.

Yih[11] defined the stream function for 3D incompressible flow. The 3D stream function is defined by the intersection of two sets of orthogonal stream surfaces with four intersection points defining a 3D streamtube. The main drawback of using this definition is the difficulty to trace the streamtube in 3D space.

Due to the complexity in tracing streamtubes, it is more efficient to trace a streamline passing through the center of the streamtube. Fay and Pratts[8] presented early works that use streamlines in 2D system.

Tracing streamlines in 3D space is based on particle tracking. The most efficient method for tracing streamlines was introduced by Pollock[12] and King & Datta-Gupta[5]. They used a piece-wise linear interpolation for the velocity field through an orthogonal gridblock. To trace streamlines through a non-orthogonal gridblock, Prevost *et al*.[13] and Cordes & Kinzelbach[14] used isoparametric transformation to transform corner-point geometry grids into orthogonal grids. They traced the streamlines in the orthogonal grids by applying the piece-wise linear interpolation technique, and then transform the exit coordinate back to physical space.

The breakthrough in streamline technology is the concept of time-of-flight (TOF). Datta-Gupta & King[15] introduced the concept of TOF to decouple the 3D saturation equation into a series of 1D equation, which can be solved more efficiently.

Many researchers[1,2,16,17] used the concept of operator splitting to include the effect of gravity and capillarity. The main idea of operator splitting is to solve the Buckley-leverett equation in two steps. First, solve the viscous forces along the streamlines using the concept of TOF. Second, solve for gravity and capillarity forces on the grids.

Osako *et al.*[18] used the concept of operator splitting to correct for the unsteady state velocity and transverse flux terms along the streamlines which has been neglected in the conventional streamline simulations.

1.2.2 Transfer Functions

There are two main approaches that have been utilized in the past to model flow through naturally fractured reservoirs. The first approach uses dual-porosity models facilitating sugar-cube type realizations, which was first introduced to the industry by Warrn and Root[19]. This model assumes two continuous media, rock matrix and fracture network. They are superimposed and interconnected by transfer functions which govern flow between the two media. This approach will yield two continuity equations for each media.

Kazemi *et al.*[20] introduced the first multiphase transfer function. Many authors[21,22,23] have reported extensive research using this type of transfer functions. In this study, we will refer to this type of transfer function as conventional transfer function (CTF). Sonier *et al.*[24] and Litvak[25] modified the CTF by including the gravitational effect due to partially water-filled fractures.

Many authors[22,26,27] modified the CTF by dividing matrix blocks into sub-domains. This technique provides pressure and saturation distributions inside the matrix-block; but it will increase the number of variables as the number of sub-domains increases.

The second approach is based on analytical and empirical models that describe the transfer between matrix-blocks and fractures[28,29,30,31,32]. These models have been coupled to Buckley-Leverett equation through a fast convolution.

Aronofsky *et al.*[33] derived an empirical transfer function to describe the mechanism of oil recovery from the porous matrix through water invasion in fractured media. Their

transfer function consisted of one exponential term. Mattax and Kyte[34] used this transfer function to fit the oil recovery data for alundum and sandstone cores, correlating their data with a dimensionless time. DeSwaan[30] coupled the empirical transfer function derived by Arnofsky *et al*.[33] with the Buckley-Leverett equation through a fast convolution to account for varying saturations in the fracture system. Kazemi *et al*.[32] modified the dimensionless time by using the concept of the shape factor. They introduced a finite difference formulation to solve the Buckley-Leverett equation proposed by DeSwaan[30]. They suggested the use of more than one exponential term to describe the transfer function.

Civan[28] derived a double-exponential-transfer function based on a rigorous theoretical analysis. Gupta & Civan[31] and Civan *et al*.[29] improved the dimensionless time by including the contact angle to account for rock wettability. They introduced an empirical transfer function with three exponential terms.

Terez and Firoozabadi[35] used an empirical formulation with only two exponential terms to account for both concurrent and countercurrent contributions to the oil recovery. They also found that the recovery from the matrix-blocks is proportional to the square root of the fracture-water saturation.

Many authors[36,37,38,39,40] derived analytical models to describe the countercurrent imbibition process. These models are base on analytical solutions for the nonlinear partial differential equation which describe the countercurrent mechanism[41]. These models require solving an infinite series of exponential terms. Dutra and Aziz[42] managed to represent the infinite series by two-term finite series which leads to a practical implementation in a large-scale simulation.

1.3 Objectives of the Study

In single porosity systems, streamline simulation has proved to be an excellent tool in modeling fluid transport in water injection processes. So far streamline simulation has not been used to model fluid flow in naturally fractured system because the current formulations don't address the fluid transfer between matrix-blocks and fractures.

The main objectives of this study are to:

1. Modify the current formulation of streamline simulation to model fluid transport in naturally fractured reservoirs under waterflooding conditions.

2. Discuss the use of different type of transfer functions to describe the fluid exchange between fracture system and matrix-blocks.

3. Derive analytical and numerical solutions for the saturation equation in terms of TOF and implement those solutions in the existing code for single-porosity streamline simulation.

4. Compare the dual-porosity streamline simulator to a commercial dual-porosity finite difference simulator, ECLIPSE.

1.4 Methodology

Four steps have been implemented to archive the objectives of this research,

1. We have derived the governing equations that describe the fluid transport in naturally fractured reservoirs. Two main equations have been derived: (1) pressure equation and (2) saturation equation. For incompressible flow, the pressure equation has been derived by adding the conservation equation for different phases and using Darcy's law. In this research, two phases has been

considered, oil and water. This equation is utilized to trace streamlines in naturally fractured reservoir. Also, it gave an important insight on how rock and fluid properties affect streamline trajectories. Saturation equation, a mass conservation equation, has been derived in terms of the streamline TOF. This equation describes saturation evolution along streamlines in naturally fractured systems. The transfer function, which describes the flow from the matrix-blocks to the fracture system, has been added to the saturation equation as a source term.

2. We have derived analytical and numerical solutions for the saturation equation. The analytical solution has been derived using Laplace transform under certain conditions. The numerical solution has been derived by writing the saturation equation in a finite-difference form.

3. We have implemented these solutions in the existing code for single-porosity streamline simulation, S3D, at Texas A&M University. This code was written originally in FORTRAN 77. It has been modified recently to FORTRAN 90 due to memory efficiency considerations.

4. We have compared the proposed dual-porosity streamline simulator and a commercial dual-porosity finite difference simulator, ECLIPSE.

1.5 Thesis Outline

This thesis consists of five chapters:

1. Chapter I gives an introduction to the research work done, the objectives of this study, and the methodology of achieving these objectives.

2. Chapter II discusses the theory behind this study. It presents the methodology by which streamline-based simulation can describe the fluid transport in naturally

fractured reservoirs. It discusses analytical and numerical solution of the saturation equation.

3. Chapter III discusses the implementation of different transfer functions. Also, it presents a comparison between the proposed dual-porosity streamline simulator and a commercial dual-porosity finite difference simulator, ECLIPSE.

4. Chapter IV summarizes the thesis with conclusions and recommendations. It presents the limitations of the proposed approach and possible improvements for future works.

CHAPTER II
THEORY

This chapter presents the development of fluid flow and transport equations in naturally fractured systems. It shows how these equations are used to reformulate the single-porosity streamline model to describe the fluid transport in dual-porosity systems. Moreover, it discusses the analytical and numerical solutions of the transport equation which describes the saturation evolution along the streamlines. Finally, it presents the methodology used to map saturation on the grid-blocks for the next pressure update.

2.1 Assumptions and Considerations

In naturally fractured reservoirs, fluids exist in two systems.

- The rock matrix, which provides the main bulk of the reservoir volume and storage.
- The highly permeable rock fractures which provide the main path for fluid flow.

If the fracture system provides the main path and storage for fluid, i.e. it is not connected to the matrix system, this can be considered as a single-porosity single-permeability system, Figure 2.1. If the fluid flow in the reservoir takes place only through the fracture networks while the matrix-blocks are linked only through the fracture system, this could be regarded as a dual-porosity single-permeability system, Figure 2.2. If there is flow between matrix-blocks, this can be considered as a dual-porosity dual-permeability system, Figure 2.3.

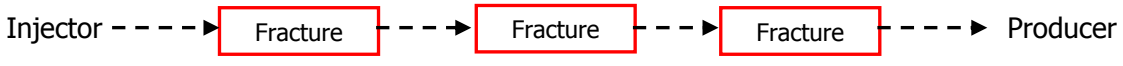

Figure 2.1-Single-Porosity Single-Permeability System.

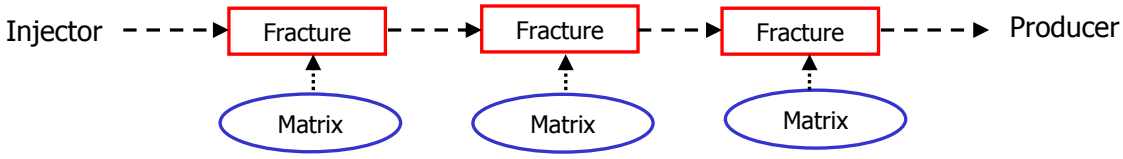

Figure 2.2-Dual-Porosity Single-Permeability System.

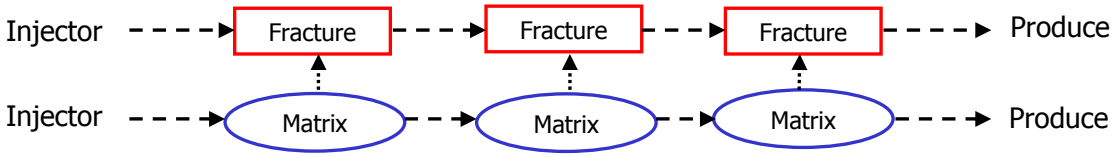

Figure 2.3-Dual-Porosity Dual-Permeability System.

This study considers the most commonly used system, the dual-porosity single-permeability system. In a dual-porosity single-permeability system, an injected fluid will not sweep out oil from the matrix-blocks. Production from the matrix-blocks can be associated with various physical mechanisms including:

- Oil expansion
- Imbibition
- Gravity imbibition/drainage
- Viscous Displacement

In this study, we consider modeling the dual-porosity single-permeability system when the imbibition and the gravity mechanisms are the most dominant forces to recover oil from the matrix-blocks.

2.2 Fluid Flow Equations in Naturally Fractured Systems

The fluid flow equations that describe fluid transport in an incompressible two phase and a dual-porosity dual-permeability system consist of two sets of equations[20,21,22,23]. The

first set of equations deals with the fluid transport in the fracture system, Eq.2.1, and the second set deals with the fluid transport in the matrix system, Eq.2.2. Each set consists of one equation for each phase.

$$\begin{aligned}\nabla \cdot k_f \cdot \left(\lambda_{of} \nabla P_{of} + \lambda_{ogf} \nabla Z_f\right) + \Gamma_o + q_{of} &= \phi \frac{\partial S_{of}}{\partial t} \\ \nabla \cdot k_f \cdot \left(\lambda_{wf} \nabla P_{wf} + \lambda_{wgf} \nabla Z_f\right) + \Gamma_w + q_{wf} &= \phi \frac{\partial S_{wf}}{\partial t}\end{aligned} \quad \text{..... (2.1)}$$

$$\begin{aligned}\nabla \cdot k_m \cdot \left(\lambda_{om} \nabla P_{om} + \lambda_{ogm} \nabla Z_f\right) - \Gamma_o + q_{om} &= \phi \frac{\partial S_{om}}{\partial t} \\ \nabla \cdot k_m \cdot \left(\lambda_{wm} \nabla P_{wm} + \lambda_{wgm} \nabla Z_m\right) - \Gamma_w + q_{wm} &= \phi \frac{\partial S_{wm}}{\partial t}\end{aligned} \quad \text{..... (2.2)}$$

The subscripts *m* and *f* represents matrix and fracture system respectively. The mobility of oil and water in each system, λ_o and λ_w, are defined, as follows:

$$\begin{aligned}\lambda_o &= \frac{k_{ro}}{\mu_o} \\ \lambda_w &= \frac{k_{rw}}{\mu_w}\end{aligned} \quad \text{..... (2.3)}$$

The gravity terms, λ_{og} and λ_{wg}, are defined, as follows:

$$\begin{aligned}\lambda_{og} &= \frac{k_{ro} \rho_o g}{\mu_o} \\ \lambda_{wg} &= \frac{k_{rw} \rho_w g}{\mu_w}\end{aligned} \quad \text{..... (2.4)}$$

The transfer terms, Γ_o and Γ_w, represent the volumetric oil and water rate transferred between fracture and matrix system.

To describe fluid transport in naturally fractured systems using the streamlines technique, each set of fluid flow equations, Eq.2.1 and Eq.2.2, has to be decoupled into two equations :(1) pressure equation and (2) saturation equation.

Solving the pressure equation will facilitate tracing the streamlines. Solving the saturation equation will describe the saturation evolution along the streamlines.

2.2.1 Pressure Equations

If we neglect capillarity and add the two phase equations for each system, we can obtain the pressure equations for fracture and matrix system.

$$\nabla \cdot k_f \cdot \left(\lambda_{tf} \nabla P_f + \lambda_{gf} \nabla Z_f \right) + \Gamma_t = -q_{sf} \quad \text{.....(2.5)}$$

$$\nabla \cdot k_m \cdot \left(\lambda_{tm} \nabla P_m + \lambda_{gm} \nabla Z_m \right) - \Gamma_t = -q_{sm} \quad \text{.....(2.6)}$$

where

$$\begin{aligned} \lambda_t &= \lambda_o + \lambda_w \\ \lambda_g &= \lambda_{og} + \lambda_{wg} \end{aligned} \quad \text{.....(2.7)}$$

The total transfer term, Γ_t, is given as:

$$\Gamma_t = \Gamma_o + \Gamma_w \quad \text{.....(2.8)}$$

Eq.2.5 and Eq.2.6 indicate that streamlines have to be traced in both fracture and matrix systems because flow occurs in both systems. In this research, we assume no flow between matrix-blocks, dual-porosity single permeability system. So, the flow and sink terms in Eq.2.6 will vanish. Eq.2.6 can be written as:

$$\Gamma_t = 0 \quad \text{.....(2.9)}$$

If we combine Eq.2.8 and Eq.2.9, we conclude that the transfer terms, Γ_o and Γ_w, have equal magnitudes and opposite directions.

$$\Gamma_o = -\Gamma_w \quad \text{.....(2.10)}$$

Since there is no flow term in the matrix system, streamlines will be generated and traced only in the fracture system. In dual-porosity single-permeability system, only one pressure equation is needed to trace the streamlines in fractures.

$$\nabla \cdot k_f \cdot \left(\lambda_{tf} \nabla P_f + \lambda_{gf} \nabla Z_f \right) = -q_{sf} \quad \text{.....(2.11)}$$

Eq.2.11 is the governing pressure equation in dual-porosity single-permeability system. It is important to point out that the transfer term doesn't appear in this equation which means that the transfer term will not affect streamlines trajectories. The pressure solution of Eq.2.11 can be used to generate a velocity field. This velocity field can be used to trace the streamlines[1,2,3,12].

2.2.2 Saturation Equations

In similar procedures done to derive the saturation equation in the single-porosity system[43], we derived two saturation equations to describe the fluid transport in the dual-porosity dual-permeability system in terms of Cartesian coordinates.

$$\phi \frac{\partial S_{wf}}{\partial t} + \vec{u}_{tf} \cdot \nabla f_{wf} + \nabla \cdot \vec{G}_f + \Gamma_w = 0 \quad \text{.....(2.12)}$$

$$\phi \frac{\partial S_{wm}}{\partial t} + \vec{u}_{tm} \cdot \nabla f_{wm} + \nabla \cdot \vec{G}_m - \Gamma_w = 0 \quad \text{.....(2.13)}$$

Eq.2.12 and Eq.2.13 assumes no capillarity in both systems. f_w is the fractional flow of water.

$$f_w = \frac{\lambda_w}{\lambda_t} \quad \text{.....(2.14)}$$

and G represents the gravity term and can be defined as,

$$\vec{G} = k \cdot \frac{\lambda_w \lambda_o}{\lambda_t} (\rho_o - \rho_w) g\vec{Z} \quad \text{.....(2.15)}$$

To write Eq.2.12 and Eq.2.13 in terms of streamline TOF, The following coordinate transformation can be applied[15]:

$$\vec{u}_t \cdot \nabla = \phi \frac{\partial}{\partial \tau} \quad \text{.....(2.16)}$$

.

The saturation equations for fracture and matrix system in terms of streamline TOF have the following form:

$$\frac{\partial S_{wf}}{\partial t} + \frac{\partial f_{wf}}{\partial \tau_f} + \frac{\nabla . \vec{G}_f}{\phi_f} + \frac{\Gamma_w}{\phi_f} = 0 \quad \text{.....(2.17)}$$

$$\frac{\partial S_{wm}}{\partial t} + \frac{\partial f_{wm}}{\partial \tau_m} + \frac{\nabla . \vec{G}_m}{\phi_m} - \frac{\Gamma_w}{\phi_m} = 0 \quad \text{.....(2.18)}$$

TOF, τ, is the time required by a tracer particle to travel along the streamline from an injector to a producer. Eq.2.17 and Eq.2.18 can be used to solve for saturation evolution along the streamlines in fracture and matrix systems.

If we assume dual-porosity single-permeability system, the convective term and gravity term in Eq.2.18 will vanish. Eq.2.18 can be rewritten in the following form:

$$\Gamma_w = \phi_m \frac{\partial S_{wm}}{\partial t} \quad \text{.....(2.19)}$$

Eq.2.19 is a simple mass conservation equation which describes the saturation changes in matrix-blocks in a dual-porosity single permeability system. The main transport equation in the dual-porosity single permeability system is Eq.2.17 because streamlines will be trace only through fractures. For the rest of the thesis, we will refer to the TOF in Eq.2.17 as τ instead of τ_f.

So far, we have shown how to derive the saturation equations for dual-porosity dual-permeability and dual-porosity single-permeability systems in terms of streamline TOF. The next step is to derive an expression for the transfer function Γ_w. we will consider only the most commonly used system which is dual-porosity single-permeability system in his study.

2.3 Matrix/Fracture Transfer Functions for Imbibition Processes

For dual-porosity single-permeability system, there are more than 20 matrix/fracture transfers functions available in the literature. In this study, we will consider three major types of matrix/fracture transfer functions: (1) conventional transfer functions (CTF), (2) diffusion transfer functions (DTF), and (3) empirical transfer functions (ETF).

2.3.1 Conventional Transfer Functions

The conventional transfer function (CTF) is the standard transfer function in commercial dual-porosity simulator. Ignoring the gravity forces and assuming a pseudo-steady state

behavior in the matrix-block, the conventional transfer function has the following form for both water and oil phases[19,20,21,22,23]:

$$\Gamma_w = F_s k_m \lambda_{wmf} \left(P_{wf} - P_{wm} \right)$$
$$\Gamma_o = F_s k_m \lambda_{omf} \left(P_{of} - P_{om} \right) \quad \text{..... (2.20)}$$

where

$$P_{wm} = P_{om} - P_{cm}$$
$$P_{wf} = P_{of} - P_{cf} \quad \text{..... (2.21)}$$

The mobility ratios, λ_{wmf} and λ_{omf}, represent the upstream mobility ratios between fracture and matrix systems.

The shape factor, F_s, is defined as follows[32]:

$$F_s = \frac{1}{V_m} \sum_s \frac{A_m}{d_m} \quad \text{..... (2.22)}$$

V_m is the volume of the matrix-block, A_m is the surface area exposed for flow between fracture and matrix system, *dm* is the distance form the exposed surface for flow to the center of the matrix block.

For a rectangular matrix block with all sides exposed to imbibing water, the shape factor has the following form[20]:

$$F_s = 4 \left(\frac{1}{l_x^2} + \frac{1}{l_y^2} + \frac{1}{l_z^2} \right) \quad \text{..... (2.23)}$$

If we apply Eq.2.9, we can find an expression for oil-pressure difference between the matrix-blocks and the fracture system.

$$\left(P_{of}-P_{om}\right)=\frac{\lambda_{wmf}}{\lambda_{omf}+\lambda_{wmf}}\left(P_{cf}-P_{cm}\right) \quad \text{..... (2.24)}$$

By substituting Eq.2.24 into Eq.2.20, we arrive at the conventional transfer function for the dual-porosity streamline simulator.

$$\Gamma_w = F_s k_m \frac{\lambda_{wmf}\lambda_{omf}}{\lambda_{wmf}+\lambda_{omf}}\left(P_{cm}-P_{cf}\right) \quad \text{..... (2.25)}$$

If we assume countercurrent imbibition mechanisms, the amount water imbibe into the matrix-blocks is equal to the amount of oil expelled from the matrix-block. The conventional transfer that describe this type of mechanism is[32,44, 45],

$$\Gamma_w = F_s k_m \frac{\lambda_{wf}\lambda_{om}}{\lambda_{wf}+\lambda_{om}}\left(P_{cm}-P_{cf}\right) \quad \text{..... (2.26)}$$

Substituting Eq.2.25 into Eq.2.17 gives

$$\frac{\partial S_{wf}}{\partial t}+\frac{\partial f_{wf}}{\partial \tau}+\frac{\nabla.\vec{G}_f}{\phi_f}+\frac{F_s k_m}{\phi_f}\frac{\lambda_{wmf}\lambda_{om}f}{\lambda_{wmf}+\lambda_{omf}}\left(P_{cm}-P_{cf}\right)=0 \quad \text{..... (2.27)}$$

Eq.2.27 represents the standard saturation equation which we solve for saturation along the streamlines. We will mainly use this equation when comparing the dual-porosity streamline simulator with the dual-porosity finite difference simulator, ECLIPSE.

2.3.2 Diffusion Transfer Functions

The partial differential equation which describes the countercurrent imbibition process in a single matrix-block with immissicible and incompressible fluid flow has the following form[41]:

$$\nabla \cdot \left[D\left(S_{wnm}\right) \nabla S_{wnm} \right] = \frac{\partial S_{wnm}}{\partial t} \quad \text{..... (2.28)}$$

$D(S_{wnm})$ is called capillary diffusivity or the diffusion coefficient.

$$D\left(S_{wnm}\right) = -\frac{k_m k_{rwm}}{\phi_m \mu_{wm}} \frac{\partial P_{cm}}{\partial S_{wnm}} \quad \text{..... (2.29)}$$

S_{wnm} is the normalized water saturation in the matrix-block.

$$S_{wnm} = \frac{S_{wm} - S_{wmc}}{1 - S_{orm} - S_{wmc}} \quad \text{..... (2.30)}$$

Initial and boundary conditions are

$S_{wnm} = 0$ at t = 0

$S_{wnm} = 1$ at boundaries

Cil *et al*.[38] derived an analytical solution for Eq.2.28 using the principle of superposition.

$$S_{wnm} = 1 - f\left(t_{Dx}\right) \cdot f\left(t_{Dy}\right) \cdot f\left(t_{Dz}\right) \quad \text{..... (2.31)}$$

t_{Dx}, t_{Dy}, and t_{Dz} are dimensionless time variables.

$$t_{Dx} = \frac{D(S_{wmn})t}{{l_x}^2}$$
$$t_{Dy} = \frac{D(S_{wmn})t}{{l_y}^2} \quad \text{.....(2.32)}$$
$$t_{Dz} = \frac{D(S_{wmn})t}{{l_z}^2}$$

$f(t_D)$ is an infinite series.

$$f(t_D) = \frac{8}{\pi^2}\sum_{n=0}^{\infty}\frac{e^{-\pi^2(2n+1)^2 t_D}}{2n+1} \quad \text{.....(2.33)}$$

Dutra and Aziz[42] simplified Eq.2.33 by replacing the infinite series by a two-term finite series.

$$f(t_D) = \frac{1}{2}\left(e^{-\xi_1 t_D} + e^{-\xi_2 t_D}\right) \quad \text{.....(2.34)}$$

They used $\xi_1 = 8.0405$ and $\xi_2 = 22.611$ by fitting Eq.2.33 to Eq.2.34 at two points. Note that ξ_1 and ξ_2 are fixed values and can be used with any value for t_D. Using the simplified series, Eq.2.31 can be written as:

$$S_{wnm} = 1 - \frac{1}{8}\sum_{n=1}^{8} e^{-\alpha_n t} \quad \text{.....(2.35)}$$

ω_n are rate constants defined as:

$$\alpha_n = D\left(S_{wnm}\right)\left(\frac{\xi_i}{L_x^2}+\frac{\xi_j}{L_y^2}+\frac{\xi_k}{L_z^2}\right) \text{where } \begin{matrix} i=1,2 \\ j=1,2 \\ k=1,2 \end{matrix} \quad \text{.....(2.36)}$$

Eq.2.35 can be used to estimate the cumulative oil recovery from a matrix-block surrounded by water.

$$Q = Q_\infty\left(1-\frac{1}{8}\sum_{n=1}^{8} e^{-\alpha_n t}\right) \quad \text{.....(2.37)}$$

Q_∞ is the ultimate oil recovery from the matrix-block.

$$Q_\infty = \left(1-S_{orm}-S_{wcm}\right)\phi_m \quad \text{.....(2.38)}$$

By differentiating Eq.2.37, the volumetric rate of water imbibed into the matrix-blocks, assuming that the fracture surface is always exposed to 100% water saturation, is

$$\Gamma_{w@\ S_{wf}=1.0} = Q_\infty\left(\frac{1}{8}\sum_{n=1}^{8}\alpha_n e^{-\alpha_n t}\right) \quad \text{.....(2.39)}$$

The effect of changing water saturation in the fracture system can be included by applying a fast convolution.

$$\Gamma_w = \frac{Q_\infty}{8}\int_0^t\left[\sum_{n=1}^{8}\alpha_n e^{-\alpha_n(t-\varepsilon)}\right]\frac{\partial S_{wf}\left(\varepsilon\right)}{\partial\varepsilon}\partial\varepsilon \quad \text{.....(2.40)}$$

By substituting Eq.2.40 into Eq.2.17,

$$\frac{\partial S_{wf}}{\partial t}+\frac{\partial f_{wf}}{\partial \tau}+\frac{\nabla\cdot\vec{G}_f}{\phi_f}+\frac{Q_\infty}{8\phi_f}\int_0^t\left[\sum_{n=1}^{8}\alpha_n e^{-\alpha_n(t-\varepsilon)}\right]\frac{\partial S_{wf}(\varepsilon)}{\partial\varepsilon}\partial\varepsilon=0 \quad \text{..... (2.41)}$$

Eq.2.41 is saturation equation for naturally fractured reservoir with a diffusion transfer function.

2.3.3 Empirical Transfer Functions

When the countercurrent imbibition process is the dominant force to displace oil from the matrix, the cumulative oil recovery from a matrix-block surrounded by water can be approximated by the following form[33]:

$$Q=Q_\infty\left(1-e^{-\omega t}\right) \quad \text{..... (2.42)}$$

ω is a rate constant which can be defined as the reciprocal of the time required by the matrix-block to expel 63% of the recoverable oil[32]. This constant can be determined empirically from laboratory experiments.

Mattax and Kyle[34] used Eq.2.42 to correlate the imbibition oil recovery data for alundum and sandstone cores imbibing from one end or all sides. They fit their data using a dimensionless time, t_{DC}, and a dimensionless rate constant, ω_{DC}.

$$t_{DC}=\left[\sqrt{\frac{k_m}{\phi_m}}\left(\frac{\sigma}{\mu_{wm}L_m^2}\right)\right]t \quad \text{..... (2.43)}$$

$$\omega_{DC}=\left[\sqrt{\frac{\phi_m}{k_m}}\left(\frac{\mu_{wm}L_m^2}{\sigma}\right)\right]\omega \quad \text{..... (2.44)}$$

These dimensionless variables can be used to scale-up laboratory experiments to field applications. Kazemi *et al*.[32] modified the dimensionless terms in Eq.2.43 and Eq.2.44 in terms of the matrix block shape factor, F_s,.

$$t_{DC} = \left[\sqrt{\frac{k_m}{\phi_m}}\left(\frac{\sigma F_s}{\mu_{wm}}\right)\right] t \quad \text{.....(2.45)}$$

$$\omega_{DC} = \left[\sqrt{\frac{\phi_m}{k_m}}\left(\frac{\mu_{wm}}{\sigma F_s}\right)\right] \omega \quad \text{.....(2.46)}$$

By differentiating Eq.2.42, the volumetric rate of water transferred from the fractures system to the matrix-blocks is given by:

$$\Gamma_{w@\ S_w=1.0} = Q_\infty \omega e^{-\omega t} \quad \text{.....(2.47)}$$

Eq.2.47 assumes 100% water saturation in the fracture system. This implies that the oil transferred from the matrix is rapidly carried away by the water flowing in the fracture system. To account for changing water saturation in the fracture, a fast convolution has been utilized as suggested by DeSwaan[30]:

$$\Gamma_w = Q_\infty \omega \int_0^t e^{-\omega(t-\varepsilon)} \frac{\partial S_{wf}(\varepsilon)}{\partial \varepsilon} \partial \varepsilon \quad \text{.....(2.48)}$$

By substituting Eq.2.48 into Eq.2.17, we arrive at the governing mass conservation equation in terms of TOF.

$$\frac{\partial S_{wf}}{\partial t} + \frac{\partial f_{wf}}{\partial \tau} + \frac{\nabla \cdot \vec{G}_f}{\phi_f} + \frac{Q_\infty}{\phi_f} \omega \int_0^t e^{-\omega(t-\varepsilon)} \frac{\partial S_{wf}(\varepsilon)}{\partial \varepsilon} \partial \varepsilon = 0 \quad \text{.....(2.49)}$$

Empirical transfer function can be expressed by more than one exponential term. For example, Eq.2.42 can be generalized to the following form:

$$Q = Q_\infty - Q_1 e^{-\omega_1 t} - Q_2 e^{-\omega_2 t} - \cdots\cdots - Q_n e^{-\omega_n t} \quad \text{.....(2.50)}$$

where

$$Q_\infty = Q_1 + Q_2 + \cdots\cdots + Q_n \quad \text{.....(2.51)}$$

Gupta and Civan[31] modeled the countercurrent imbibition process as a series of exchange processes between the dead-end pore spaces in the matrix, network of interconnected pores in the matrix, and matrix/fracture interface. They derived a three exponent expression for the cumulative oil transferred into the fracture system. As follows,

$$Q = Q_\infty \left(1 - a_1 e^{-\omega_1 t} - a_2 e^{-\omega_2 t} - a_3 e^{-\omega_3 t}\right) \quad \text{.....(2.52)}$$

where a_1, a_2, a_3, ω_1, ω_2 and ω_3 are constants which can be determined empirically from lab data. Gupta and Civan[31]outlined how to calculate these constants. Also, Q_∞ represents the recoverable oil contained initially in the interconnected and dead-end pores of the matrix. Gupta and Civan[31] modified the dimensionless time, t_{DC}, and the dimensionless rate constants, ω_{iD}, by adding the contact angle, θ.

$$t_{DC} = \left[\sqrt{\frac{k_m}{\phi_m}}\left(\frac{\sigma\cos(\theta)F_s}{\mu_{wm}}\right)\right]t \quad \text{.....(2.53)}$$

$$\omega_{iD} = \left[\sqrt{\frac{\phi_m}{k_m}}\left(\frac{\mu_{wm}}{\sigma\cos(\theta)F_s}\right)\right]\omega_i, i = 1,2,3 \quad \text{..... (2.54)}$$

Following the same procedure discussed in the single exponent transfer function, we can write the volumetric oil transferred from the matrix to the fracture as follows:

$$\Gamma_w = Q_\infty \int_0^t \sum_{i=1}^{3} a_i \omega_i e^{-\omega(t-\varepsilon)} \frac{\partial S_{wf}(\varepsilon)}{\partial \varepsilon} \partial\varepsilon \quad \text{..... (2.55)}$$

By substituting Eq.2.55 into Eq.2.17, the saturation equation can be written as:

$$\frac{\partial S_{wf}}{\partial t} + \frac{\partial f_{wf}}{\partial \tau} + \frac{\nabla \cdot \vec{G}}{\phi_f} + \frac{Q_\infty}{\phi_f} \int_0^t \left[\sum_{i=1}^{3} a_i \omega_i e^{-\omega(t-\varepsilon)}\right] \frac{\partial S_{wf}(\varepsilon)}{\partial \varepsilon} \partial\varepsilon = 0 \quad \text{..... (2.56)}$$

Many authors[35,46,47] showed that countercurrent imbibition may not be enough to describe the oil recovery from matrix-blocks when the water level advances in the fracture. Countercurrent process is the only imbibbition process when the matrix-block is completely immersed in water. Prior to a complete immersion in water, the oil recovery is a result of both concurrent and countercurrent processes. The cumulative oil recovery from the matrix-blocks can be given by the following form:

$$Q = Q_\infty - Q_1 e^{-\omega_1 t} - Q_2 e^{-\omega_2 t} \quad \text{..... (2.57)}$$

where

$$Q_\infty = Q_1 + Q_2 \quad \text{..... (2.58)}$$

Q_1 and Q_2 represent the ultimate oil recovery from concurrent and countercurrent imbibition processes respectively. By differentiating Eq.2.57, the volumetric water rate transferred from the fracture system can be written as:

$$\Gamma_{w@\ S_{wf}=1.0} = Q_1\omega_1 e^{-\omega_1 t} + Q_2\omega_2 e^{-\omega_2 t} \quad \text{..... (2.59)}$$

Eq.2.59 assumes 100% water saturation in the fracture system. Terez and Firoozabadi[35] showed that for water saturation less than unity, the volumetric water rate can be given as:

$$\Gamma_{w@\ S_{wf}\le 1.0} = \left(S_{wf}\right)^m \Gamma_{w@\ S_{wf}=1.0} \quad \text{..... (2.60)}$$

They performed a sensitivity analysis to find the value of m. Based on their analysis, they found that m = 0.5. The effect of changing water saturation can be accounted for by using a fast convolution.

$$\Gamma_w = \int_0^t \left(Q_1\omega_1 e^{-\omega_1(t-\varepsilon)} + Q_2\omega_2 e^{-\omega_2(t-\varepsilon)}\right) \frac{\partial {S_{wf}}^{0.5}(\varepsilon)}{\partial \varepsilon} \partial\varepsilon \quad \text{..... (2.61)}$$

By substituting Eq.2.61 into Eq.2.17, we arrive at the governing saturation equation in naturally fractured reservoir which takes care of both cocurrent and countercurrent imbibition processes.

$$\frac{\partial S_{wf}}{\partial t} + \frac{\partial f_{wf}}{\partial \tau} + \frac{\nabla.\vec{G}}{\phi_f} + \frac{1}{\phi_f}\int_0^t \left[\sum_{i=1}^{2} Q_i\omega_i e^{-\omega_i(t-\varepsilon)}\right] \frac{\partial {S_{wf}}^{0.5}(\varepsilon)}{\partial \varepsilon} \partial\varepsilon = 0 \quad \text{..... (2.62)}$$

2.4 Matrix/Fracture Transfer Function for Gravity/Imbibition Process

In the previous section, we discussed the development of the saturation equation when the imbibition process is the most dominant force to recover oil from the matrix-block. The imbibtion process is dominant when the vertical dimension, l_z, of the matrix-block is small. If l_z is large, a gravity head between the matrix-block and the fracture system also will cause fluid movement. Figure 2.4 illustrates the gravity head concept in a single matrix-block surrounded by fractures.

The pressure difference due to the gravity head is[24,25]

$$\Delta P_{gh} = l_z \left(S_{wnf} - S_{wnm} \right)\left(\rho_w - \rho_o \right) g$$
$$S_{wnf} = \frac{S_{wf} - S_{wcf}}{1 - S_{orf} - S_{wcf}} \qquad \text{.....(2.63)}$$
$$S_{wnm} = \frac{S_{wf} - S_{wcm}}{1 - S_{orm} - S_{wcm}}$$

where S_{wnf}, S_{wnm} are the normalized water saturation in the fracture system and the matrix-block.

If gravity is considered in the development of the transfer function, the volumetric oil and water rate can be expressed as,

$$\Gamma_w = F_s k_m \lambda_{wmf} \left(P_{of} - P_{om} - P_{cf} + P_{mf} + \frac{\Delta P_{gh}}{2} \right)$$
$$\Gamma_o = F_s k_m \lambda_{omf} \left(P_{of} - P_{om} - \frac{\Delta P_{gh}}{2} \right) \qquad \text{.....(2.64)}$$

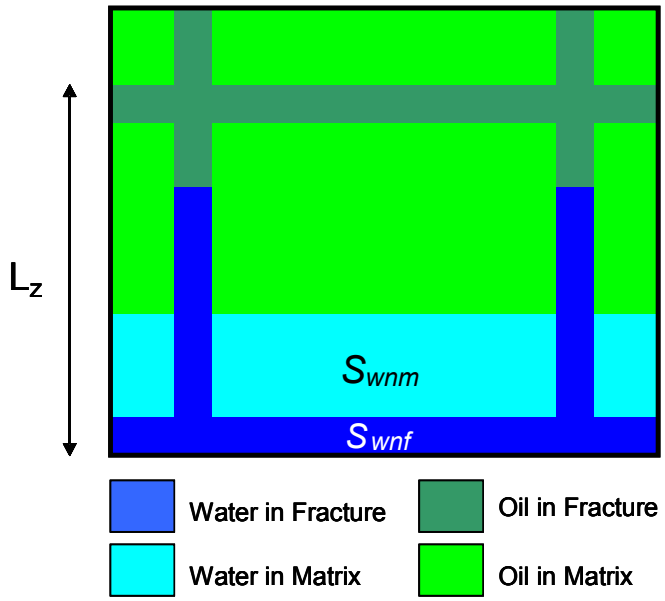

Figure 2.4-Gravity Effect in a Single Matrix-Block Surrounded by Fractures Partially Filled with Water.

Utilizing Eq.2.9, the volumetric water transfer rate between fracture and matrix system is

$$\Gamma_w = F_s k_m \frac{\lambda_{wmf}\lambda_{omf}}{\lambda_{wmf}+\lambda_{omf}}\left(P_{cm} - P_{cf} + \Delta P_{gh}\right) \quad \text{..... (2.65)}$$

Substituting Eq.2.65 into Eq.2.17 yields

$$\frac{\partial S_{wf}}{\partial t} + \frac{\partial f_{wf}}{\partial \tau} + \frac{\nabla.\vec{G}_f}{\phi_f} + \frac{F_s K_m}{\phi_f}\frac{\lambda_{wmf}\lambda_{omf}}{\lambda_{wmf}+\lambda_{omf}}\left(P_{cm} - P_{cf} + \Delta P_{gh}\right) = 0 \quad \text{..... (2.66)}$$

Eq.2.66 is the saturation equation which describes the saturation evolution in the fracture system when gravity/imbibition processes are the most dominant recovery mechanisms.

In this section, we showed how to add gravity effect to the CTF. It is also possible to add gravity effects to ETF and DTF by using a methodology proposed by Coats[44] and utilized later by Dutra and Aziz[42].

2.5 Analytical Solution for the Saturation Equation with ETF

The saturation equation with ETF and DTF can be solved analytically because the transfer function is a function only of the water saturation in the fracture system only. On the other hand, the saturation equation with CTF can't be solved analytically because the transfer function is not only a function of fracture-water saturation, but also it is a function of matrix-water saturation. In this section, we will derive the analytical solution of the saturation equation with one-exponent ETF, Eq.2.48. The analytical solution of the saturation equation with three-exponent ETF and DTF can be derived follwoing similar procedures.

If gravity and capillarity forces are ignored in the fracture system, Eq.2.48 can be rewritten in the following form:

$$\frac{\partial S_{wf}}{\partial t} + H\frac{\partial S_{wf}}{\partial \tau} + \frac{Q_\infty}{\phi_f}\omega\int_0^t e^{-\omega(t-\varepsilon)}\frac{\partial S_{wf}(\varepsilon)}{\partial \varepsilon}\partial\varepsilon = 0$$
$$H = \frac{\partial f_{wf}}{\partial S_{wf}} \qquad \text{.....(2.67)}$$

with the following initial and boundary conditions:

$$S_{wf}(\tau,0) = 0$$
$$S_{wf}(0,t) = 1 \qquad \text{.....(2.68)}$$

If we assume H is constant, we can apply Laplace transform on Eq.2.67 and transform it to s-domain. After applying the boundary conditions on the transformed equation, the water saturation in the fracture system can be given as

$$S_{wf}(\tau,s) = e^{-\tau s/H}\left[\frac{1}{s}\left(e^{-\beta s/(s+\omega)}\right)\right]$$
$$\beta = \frac{Q_\infty \omega}{\phi_f}\frac{\tau}{H} \quad \text{.....(2.69)}$$

We can use Stehfest's numerical Laplace inversion algorithm to calculate fracture-water saturation in time domain. On the other hand, we can use Laplace inverse table to invert Eq.2.69 to time-domain and arrive at the following analytical form:

$$S_{wf}(\tau,t) = 0, \qquad \tau > t \quad \text{.....(2.70)}$$

$$S_{wf}(\tau,t) = e^{-\beta}e^{-\omega(t-\tau/H)}I_0\left[2\sqrt{\beta\omega(t-\tau/H)}\right] + \Psi, \qquad \tau \le t$$
$$\Psi = \omega e^{-\beta}\int_{\tau/H}^{t} e^{-\omega(\varepsilon-\tau/H)}I_0\left[2\sqrt{\beta\omega(\varepsilon-\tau/H)}\right]\partial\varepsilon \quad \text{.....(2.71)}$$

Eq.2.70 and Eq.2.71 are similar to the analytical solution derived by Kazemi *et. al*[32] for 1D Buckley-Leverett equation in naturally fractured reservoirs. Our analytical solution is more general and can be applied to 3D problems.

Note that Ψ is an integral term which can be solved numerically. We derived an analytical solution for this integral in the following form:

$$\Psi = \omega e^{-\beta} \sum_{n=0}^{\infty} \left\{ \begin{array}{l} \dfrac{\beta^n \omega^n}{(n!)^2} e^{-\omega(t-\tau/H)} \\ \left[\displaystyle\sum_{m=0}^{n} (-1)^{n-m} \frac{n!(t-\tau/H)^m}{(-\omega)^{(n-m+1)} m!} + (-1)^{n+1} \frac{n!}{(-\omega)^{n+1}} \right] \end{array} \right\} \quad \text{..... (2.72)}$$

So Ψ becomes an infinite series which can be approximated using a limited number of n-values. Appendix-I discusses the development of Eq.2.72.

This analytical solution assumes that H is constant which is not always true. To overcome this shortcoming, an iterative method proposed by Shenawi *et al.*[48] can be used. In this study, we will assume H to be equal to 1, and we will use Eq.2.63 to validate the numerical solution of Eq.2.41.

2.6 Numerical Solution of the Saturation Equation

Using the concept of operator-splitting, the saturation equation, Eq.2.17, can be divided into two terms: convective term and gravity term.

The convective term has the following expression:

$$\frac{\partial S_{wf}^{c}}{\partial t} + \frac{\partial f_{wf}}{\partial \tau} + \frac{\Gamma_w}{\phi_f} = 0 \quad \text{..... (2.73)}$$

This term describes the viscous forces effect along the streamlines. It will be solved numerically along the streamlines. The saturation from Eq.2.17 will be updated using the gravity term which will be solved numerically on the grid-blocks. The gravity term has the following form:

$$\frac{\partial S_{wf}}{\partial t} + \frac{\nabla . \vec{G}_f}{\phi_f} = 0 \quad \text{..... (2.74)}$$

In single porosity system, the convective term has to be solved first. The gravity term will use saturation of the convective term as an initial condition. The same procedures are still valid in dual-porosity system.

In this section, I will discuss the numerical solution of the convective term because unlike the single porosity systems, it has the transfer function. The numerical solution of the gravity term is similar to the numerical solution of this term in single-porosity systems.

2.6.1 Numerical Solution for the Saturation Equation with CTF

The convective term of the saturation equation with CTF is

$$\frac{\partial S_{wf}^{c}}{\partial t}+\frac{\partial f_{wf}}{\partial \tau}+\frac{F_s k_m}{\phi_f}\frac{\lambda_{wmf}\lambda_{omf}}{\lambda_{wmf}+\lambda_{omf}}\left(P_{cm}-P_{cf}\right)=0 \quad \text{..... (2.75)}$$

The explicit numerical form of Eq.2.75 is

$$S_{wf,i}^{n+1}-S_{wf,i}^{n}=-\Delta t\left\{\begin{array}{l}\dfrac{f_{wf,i}^{n}-f_{wf,i-1}^{n}}{\Delta\tau}+\\ \left(\dfrac{F_s k_m}{\phi_f}\right)_i\left(\dfrac{\lambda_{wmf}\lambda_{omf}}{\lambda wmf+\lambda omf}\right)_i^{n}\left(P_{cm}-P_{cf}\right)_i^{n}\end{array}\right\} \quad \text{..... (2.76)}$$

Matrix saturation can be calculated from the mass conservation equation, Eq.2.19. The explicit numerical form of this equation is

$$S_{wm,i}^{n+1}-S_{wm,i}^{n}=-\Delta t\left\{\left(\frac{F_s k_m}{\phi_m}\right)_i\left(\frac{\lambda_{wmf}\lambda_{omf}}{\lambda wmf+\lambda omf}\right)_i^{n}\left(P_{cm}-P_{cf}\right)_i^{n}\right\} \quad \text{..... (2.77)}$$

2.6.2 Numerical Solution for the Saturation Equation with ETF and DTF

In this section, we will discuss the numerical solution of the saturation equation with one-exponent ETF, Eq.2.48. The same methodology can be applied to derive a numerical solution of the saturation equation with three-exponent ETF and DTF.

The convective term of Eq.2.48 is

$$\frac{\partial S_{wf}}{\partial t}+\frac{\partial f_{wf}}{\partial \tau}+\frac{Q_{\infty}}{\phi_f}\omega\int_0^t e^{-\omega(t-\varepsilon)}\frac{\partial S_{wf}(\varepsilon)}{\partial \varepsilon}\partial\varepsilon=0 \quad \text{..... (2.78)}$$

To find a numerical form for Eq.2.78, we used a finite-difference scheme proposed by Kazemi *et al.*[32].

$$S_{wf,i}^{n+1}-S_{wf,i}^{n}=-\left(\frac{1}{\Delta t}+\frac{Q_{\infty}\omega}{\phi_f}e^{-\omega\Delta t}\right)^{-1}\left(\frac{f_{wf,i}^{n}-f_{wf,i}^{n}}{\Delta\tau}+\frac{Q_{\infty}\omega}{\phi_f}SUM^{\,n-1}e^{-\omega\Delta t}\right)$$

$$SUM^{\,n-1}=\left[SUM^{\,n-2}+\left(S_{wf,i}^{n}-S_{wf,i}^{n-1}\right)\right]e^{-\omega\Delta t},\qquad n\geq 1$$

$$SUM^{\,-1}=0$$

..... (2.79)

The recurrent method was used to estimate the convolution term in Eq.2 70. The recurrent method has a first order error. Luan[49] proposed different methods to reduce the error in estimating the convolution term.

Matrix saturation equation, Eq.2.19, can be solve numerically in using similar procedure

$$S_{wm,i}^{n+1}-S_{wm,i}^{n}=-\Delta t\left(\frac{Q_{\infty}\omega}{\phi_m}SUM^{\,n-1}e^{-\omega\Delta t}\right) \quad \text{..... (2.80)}$$

2.7 Saturation Mapping

In single porosity streamline simulation, pressure has to be updated to account for changing well conditions, changing mobility ratios, and gravity effects. Updating the pressure solution will require mapping the streamline saturation on the grid-blocks. In dual porosity streamline simulation, we need to map both the saturation of the fracture system and the matrix-blocks.

Mapping fracture saturation is similar to the mapping of saturation in single-porosity streamline simulation. We used the following weighted average function to map fracture saturation:

$$S_{wf,grid} = \frac{\sum_{i=1}^{nsl} S_{wf,i}\Delta\tau_i}{\sum_{i=1}^{nsl}\Delta\tau_i} \quad \text{.....(2.81)}$$

where nsl is the number of streamlines passing through a grid-block, $\Delta\tau$ is the time of flight required by a streamline to pass through the grid-block.

Matrix saturation along streamlines can be mapped on the grid-blocks using the following arithmetic average equation:

$$S_{wm,grid} = \frac{1}{nsl}\sum_{i=1}^{nsl} S_{wm,i} \quad \text{.....(2.82)}$$

If Eq.2.79 were used to solve the saturation evolution, the summation term, SUM^{n-1}, has to be mapped on the grid-block for the next time update calculations. A weighted average can be used to map the summation term.

$$SUM_{grid}^{n-1} = \frac{\sum_{i=1}^{nsl} SUM_i^{n-1} \Delta\tau_i}{\sum_{i=1}^{nsl} \Delta\tau_i} \quad \text{.....(2.83)}$$

CHAPTER III
RESULTS AND DISCUSSION

This chapter discusses the implementation of the dual-porosity streamline simulator (DPSS) with ETF, DTF and CTF. It presents a comparison between the DPSS and the fully implicit dual-porosity ECLIPSE (FIDPE) in terms of water cut, recovery, fracture water saturation, and matrix water saturation. Also, it illustrates the differences between the DPSS, the FIDPE, and the IMPES dual-porosity ECLIPSE (IMPESDPE) in terms of handling the saturation evolution in both fracture and matrix systems. Finally, it presents a comparison in CPU time for DPSS, FIDPE, and IMPESDPE.

3.1 Validating the Numerical Solution of the Saturation Equation with ETF

Since the saturation equations with ETF and DTF have a convolution term, it is important to make sure that the numerical solutions of these equations are accurate. In this section, we compare the numerical and analytical solutions of the saturation equation with one-exponent ETF, Eq.2.41. The example used to perform this comparison is a heterogeneous quarter five-spot pattern. The permeability field was generated by a discrete fracture modeling. Figure 3.1 shows a 2D permeability field which represents the fracture distribution. Other parameters are presented in Table 3.1.

Figure 3.2 shows the fracture-water saturation at different time for the numerical and the analytical solutions. The results are in excellent agreement which indicate that the numerical solution of the saturation equation is accurate.

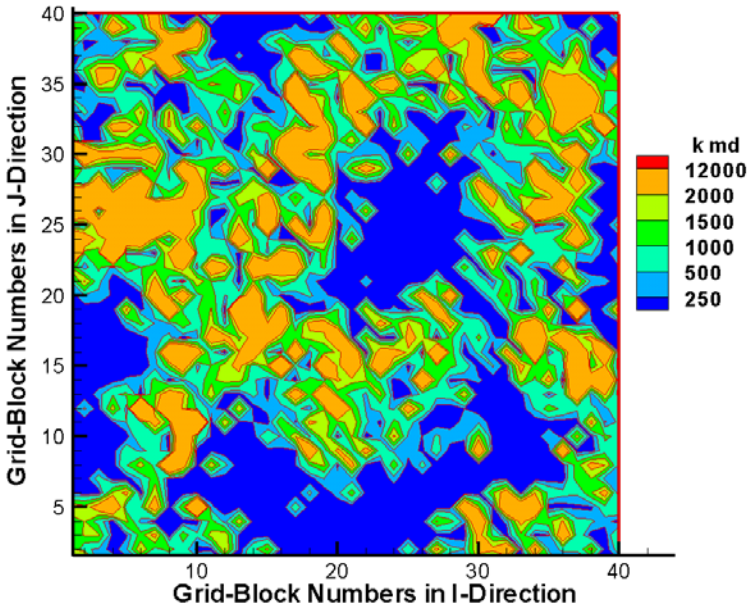

Figure 3.1-2D Permeability Field.

Table 3.1-Field Parameters for Quarter Five Spot Example Used to Validate the Numerical Solution of the Saturation Equation with ETF.

Parameters	Values
Area, ft^2	1440000
Thickness, ft	30
Injection and Production Rates, STB/Day	100
ω, 1/Day	0.001
ϕ_f	0.01
ϕ_m	0.16
S_{wcm} & S_{orm} S	0.25
k_{rwf}	S_{wf}
k_{rof}	1- S_{wf}
μ_w	1
μo	1
k_f, md	10000

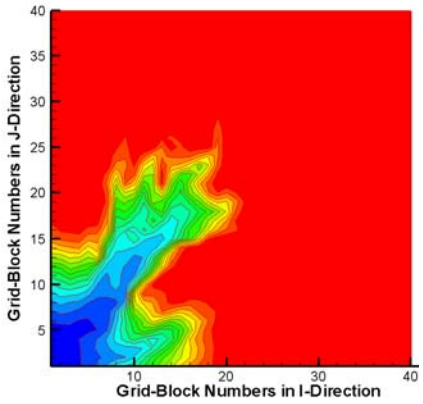

Numerical Solution at 100 days

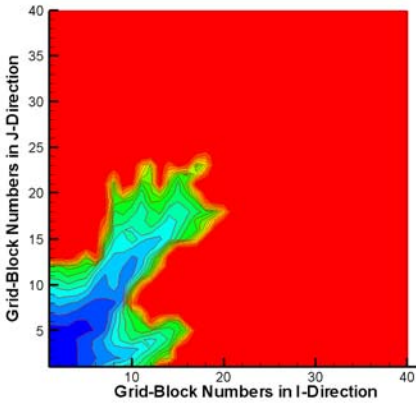

Analytical Solution at 100 days

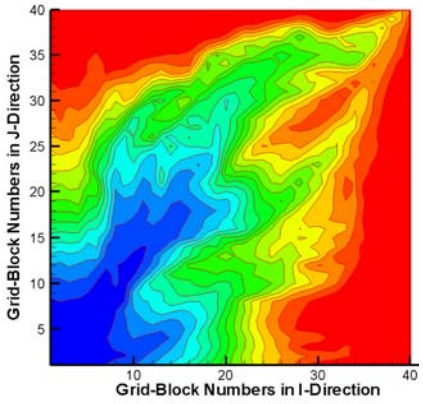

Numerical Solution at 1500 days

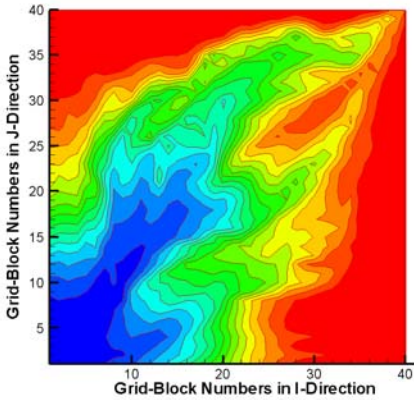

Analytical Solution at 1500 days

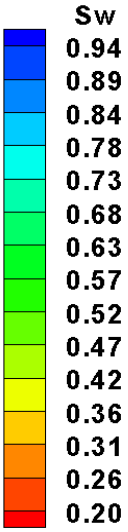

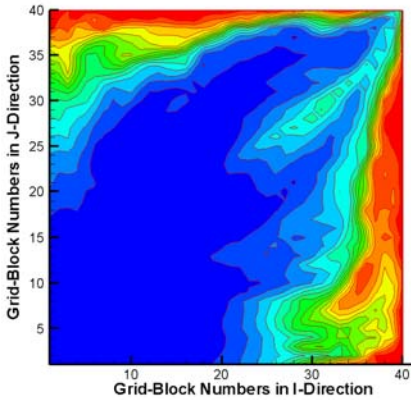

Numerical Solution at 6000 days

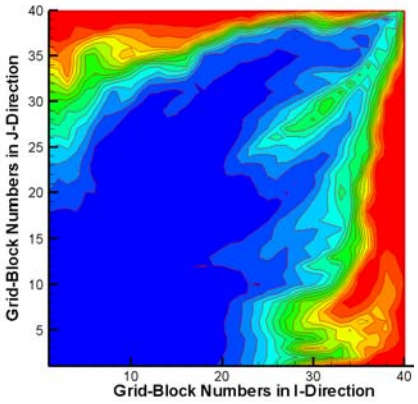

Analytical Solution at 6000 days

Figure 3.2-Comparison between the Numerical and Analytical Solutions of the Saturation Equation with ETF.

3.2 Dual-Porosity Streamline (Imbibition Mechanism)

This section presents the dual-porosity streamline simulator results when the imbibition process is the most dominant recovery mechanism. Three type of transfer functions were implemented in the existing single porosity streamline code. DPSS results were compared to FIDPE results. The comparison was based on two examples: a homogenous quarter five spot pattern, a heterogeneous quarter five-spot pattern.

3.2.1 Homogenous Case: Quarter Five Spot Pattern

This example was first presented by Kazemi *et a.l*[20] and later used by Thomas *et al.*[23] and Dutra and Aziz[42]. Table 3.2 shows the field parameters. Figure 3.3 and Figure 3.4 shows relative permeability and capillary pressure curves.

Using the DPSS with CTF is easy and direct because we have all data to describe the fluid transport in this field. On the other hand, using the DPSS with ETF and DTF is not direct because ETF and DTF depend on imbibition data from lab experiments. ETFs, Eq.2.48 and Eq.2.55, need a value for the rate constants, ω, and DTF, Eq.2.40, needs a value for the diffusive coefficient, D (S_{wm}). One way to overcome this difficulty is to solve Eq.2.28 numerically for average saturation in the matrix-block. Then, use this result to estimate the rate constants in Eq.2.48 and Eq.2.55, and the diffusive coefficient in Eq.2.40. Dutra and Aziz[42] used this technique to estimate the diffusive coefficient in Kazemi *et al.*[20] example. They found out that the diffusive coefficient that best represents this example is 0.045 ft^2/Day. We used their value in our study. To estimate the rate constants in Eq.2.48 and Eq.2.55, we matched the matrix cumulative oil recovery from Eq.2.42 and Eq.2.52 to the matrix cumulative oil recovery from Eq.2.37. Figure 3.5 shows that we have obtained an excellent match. Table 3.3 and Table 3.4 show the estimated values used to get the match. To compare the results of ETF and DTF, we run this example for 2000 days. Figure 3.6 shows almost identical results for the DPSS with ETF and DTF in terms of water cut. Figure 3.7 shows the streamlines in this example.

Table 3.2-Quarter Five Spot Parameters, Homogenous Case, Imbibition Process.

Parameters	Values
Dimension In I-Direction, ft	600
Dimension In J-Direction, ft	600
Thickness, ft	30 ft
Reservoir Grid	40 × 40×1
Injection Rates, STB/Day	210
Production Rate, STB/Day	200
k_m, md	1
k_f, md	10000
F_s, ft^2	0.08
ϕ_f	0.01
ϕ_m	0.19
μ_w, cp	0.5
μ_o, cp	3
ρ_w, psi/ft	0.44
ρ_o, psi/ft	0.3611
P_i, psi	396.89

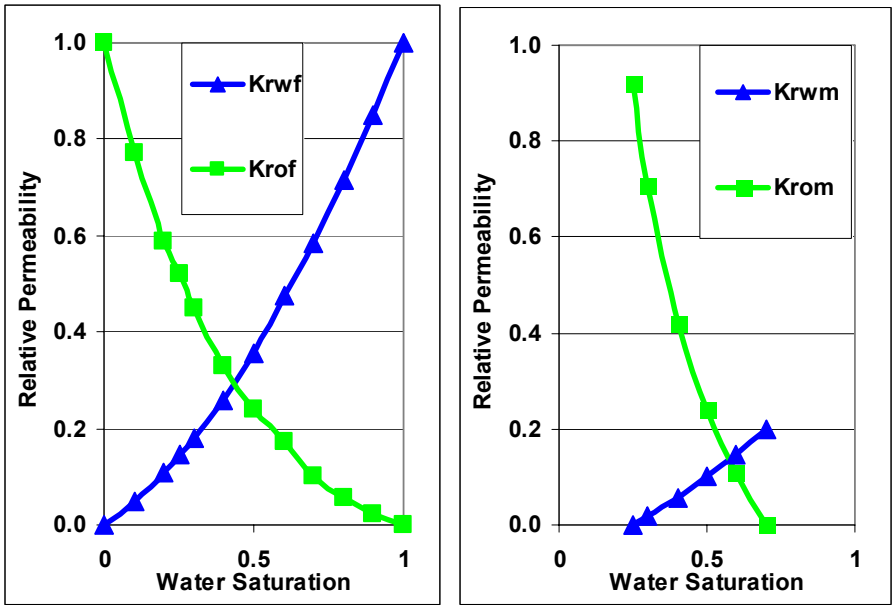

Fracture Matrix

Figure 3.3-Fracture and Matrix Relative Permeability Curves.

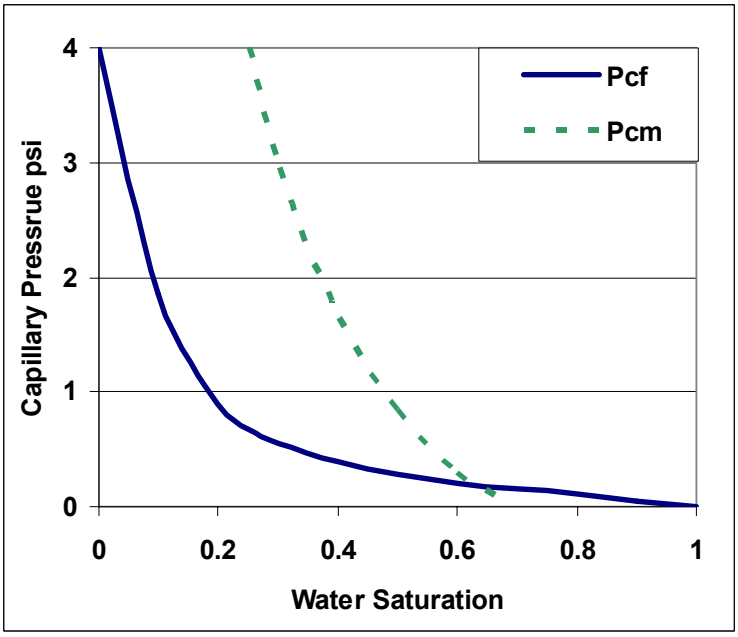

Figure 3.4-Fracture and Matrix Capillary Pressure Curves.

Table 3.3-Parameters for the Saturation Equation with One-Exponent ETF.

Parameters	Values
ω, 1/Day	0.011

Table 3.4-Parameters for the Saturation Equation with Three-Exponent ETF.

Parameters	Values
ω_1, 1/Day	8.40
ω_2, 1/Day	0.087
ω_3, 1/Day	0.0115
a_1	0.0542
a_2	0.0429
a_3	0.903

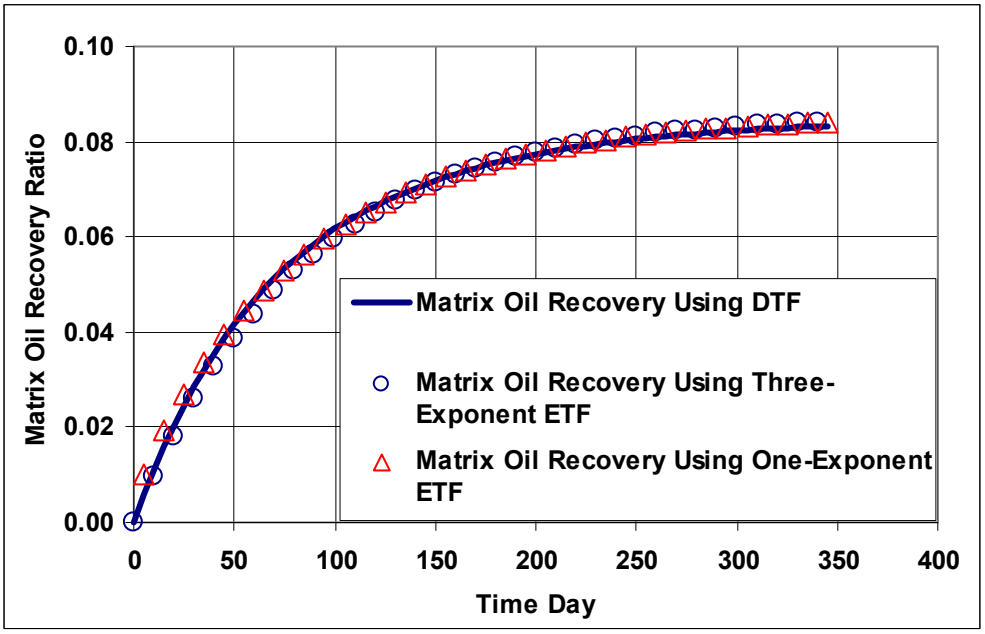

Figure 3.5-Matrix Oil Recovery Using DTF and ETF.

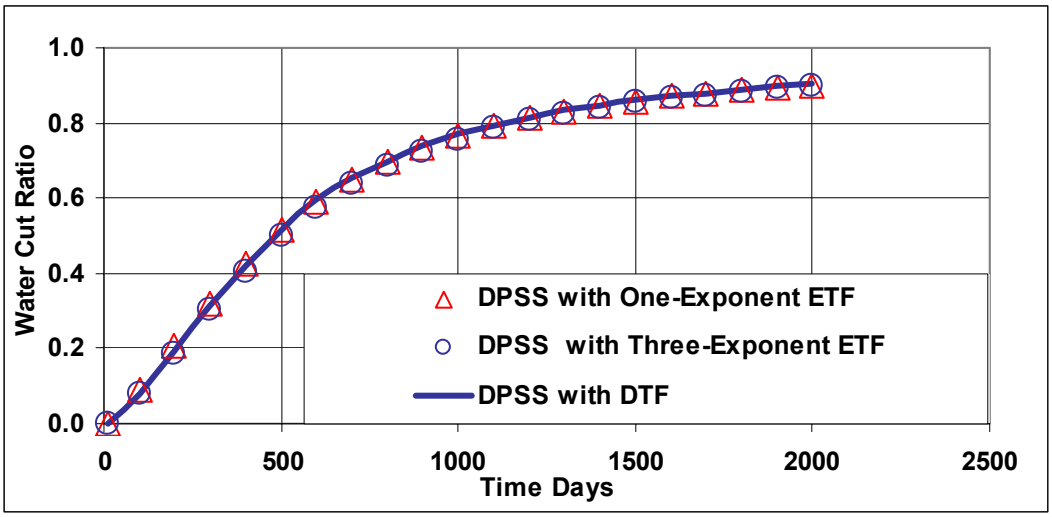

Figure 3.6-Water Cut History Using DPSS with DTF and ETE

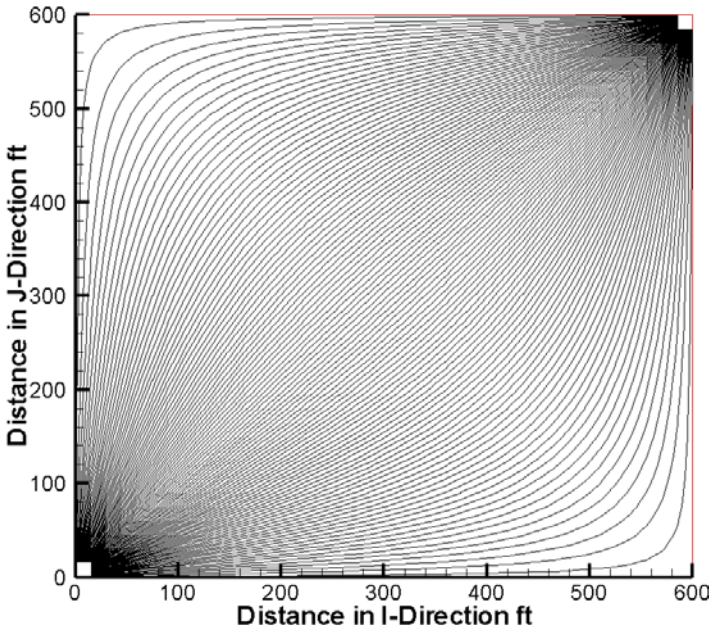

Figure 3.7-Streamlines in a Quarter Five Spot Pattern, Homogenous Case, Imbibition Process.

.

Before comparing our DPSS to FIDPE, we would like to investigate the impact of the transfer function. Figure 3.8 and Figure 3.9 shows the water saturation map and the water cut history for the DPSS with and without the CTF. For the case without CTF, water cut history is higher and the water saturation advances faster because the interaction with the matrix system is not considered. The next step is to compare the DPSS to the FIDPE. Figure 3.10 and Figure 3.11 show a comparison between DPSS and FIDPE in terms of water cut and recovery responses. The DPSS with CTF shows an excellent match with FIDPE, while DPSS with ETF and DTF shows high water cut and low recovery. These results can be confirmed by looking at the water saturation in fracture and matrix system at different time. Figure 3.12 and Figure 3.13 show a comparison between DPSS with CTF, DTF and ETF with FIDPE in terms of fracture and matrix water saturation. Fracture and matrix water saturation maps from DPSS with CTF are in good agreements with those from FIDPE. Fracture and matrix water saturation maps from DPSS with DTF and ETF shows that the water advances faster which validate water cut and recovery results.

It is important to point out that these results do not mean that the DPSS with CTF is more accurate than the DPSS with ETF and DTF. The FIDPE uses CTF to describe the fluid exchange between fracture system and matrix-blocks, and this is the reason that we have good agreements between the DPSS with CTF and the FIDPE. It is not the scope of this study to investigate the accuracy of the transfer functions. We will limit the comparisons in the next sections between the DPSS with CTF and the FIDPE because they use the same transfer function.

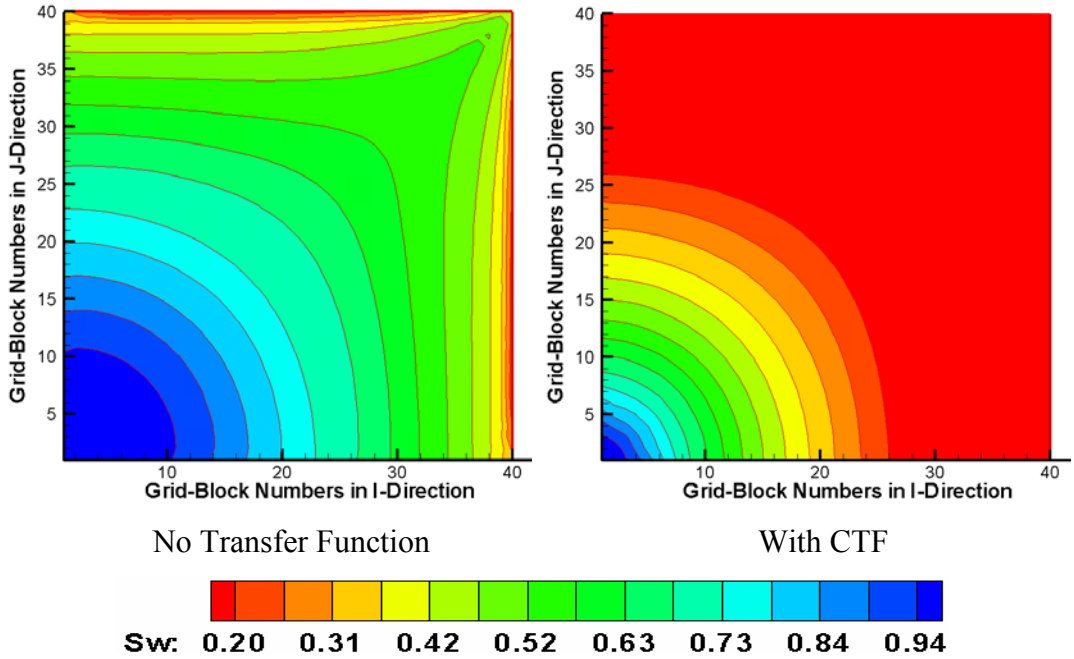

Figure 3.8-Comparison between DPSS with and without CTF in Terms of Fracture Water Saturation at 100 days, Homogenous Case, Imbibition Process.

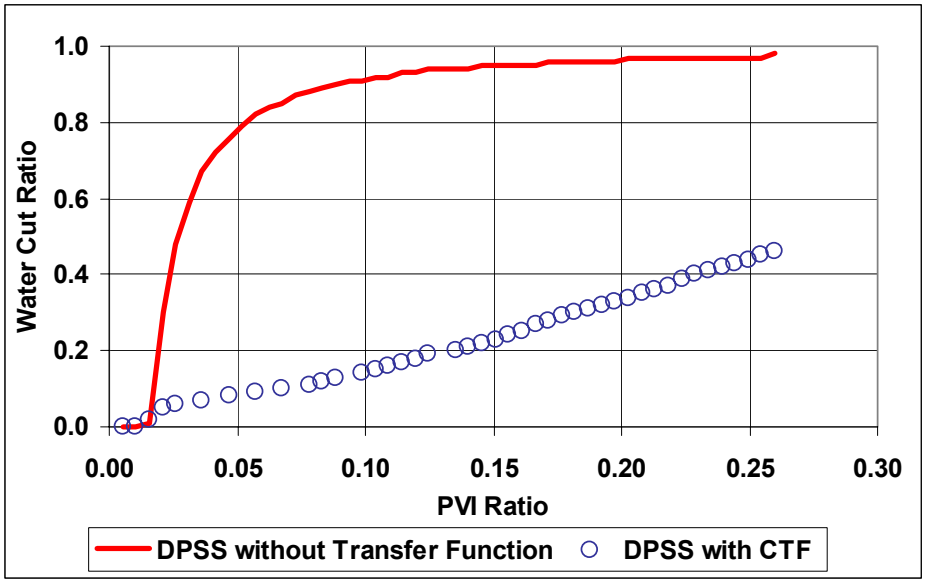

Figure 3.9-Comparison between DPSS with and without CTF in Terms of Water Cut History, Homogenous Case, Imbibition Process.

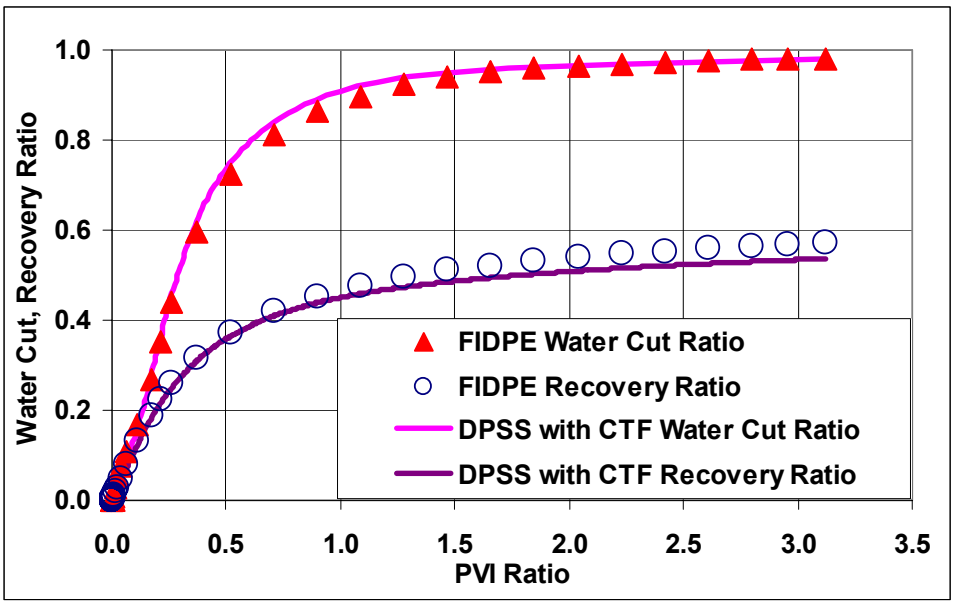

Figure 3.10-Comparison between FIDPE and DPSS with CTF in Terms of Water Cut and Recovery Histories, Homogenous Case, Imbibition Process.

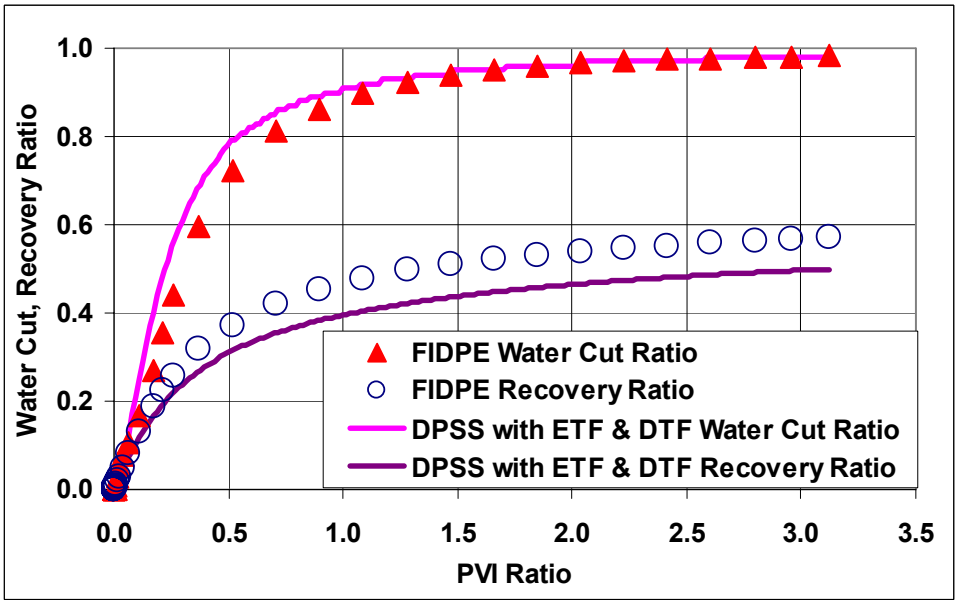

Figure 3.11-Comparison between FIDPE and DPSS with ETF and DTF in Terms of Water Cut and Recovery Histories, Homogenous Case, Imbibition Process.

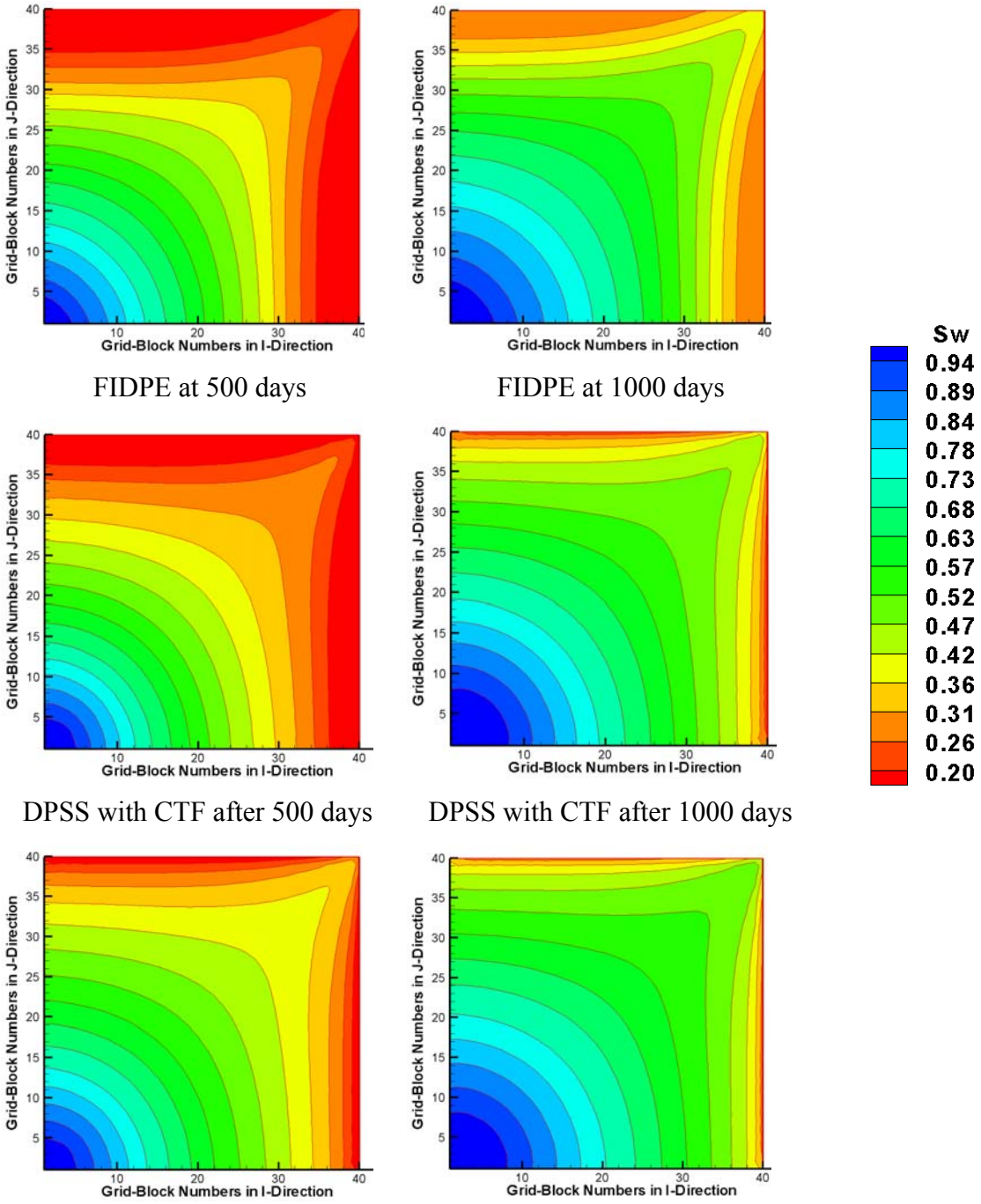

FIDPE at 500 days FIDPE at 1000 days

DPSS with CTF after 500 days DPSS with CTF after 1000 days

DPSS with ETF/ DTF at 500 days DPSS with ETF/ DTF at 1000 days

Figure 3.12-Comparison between DPSS and FIDPE in Terms of Fracture Water Saturation, Homogenous Case, Imbibition Process.

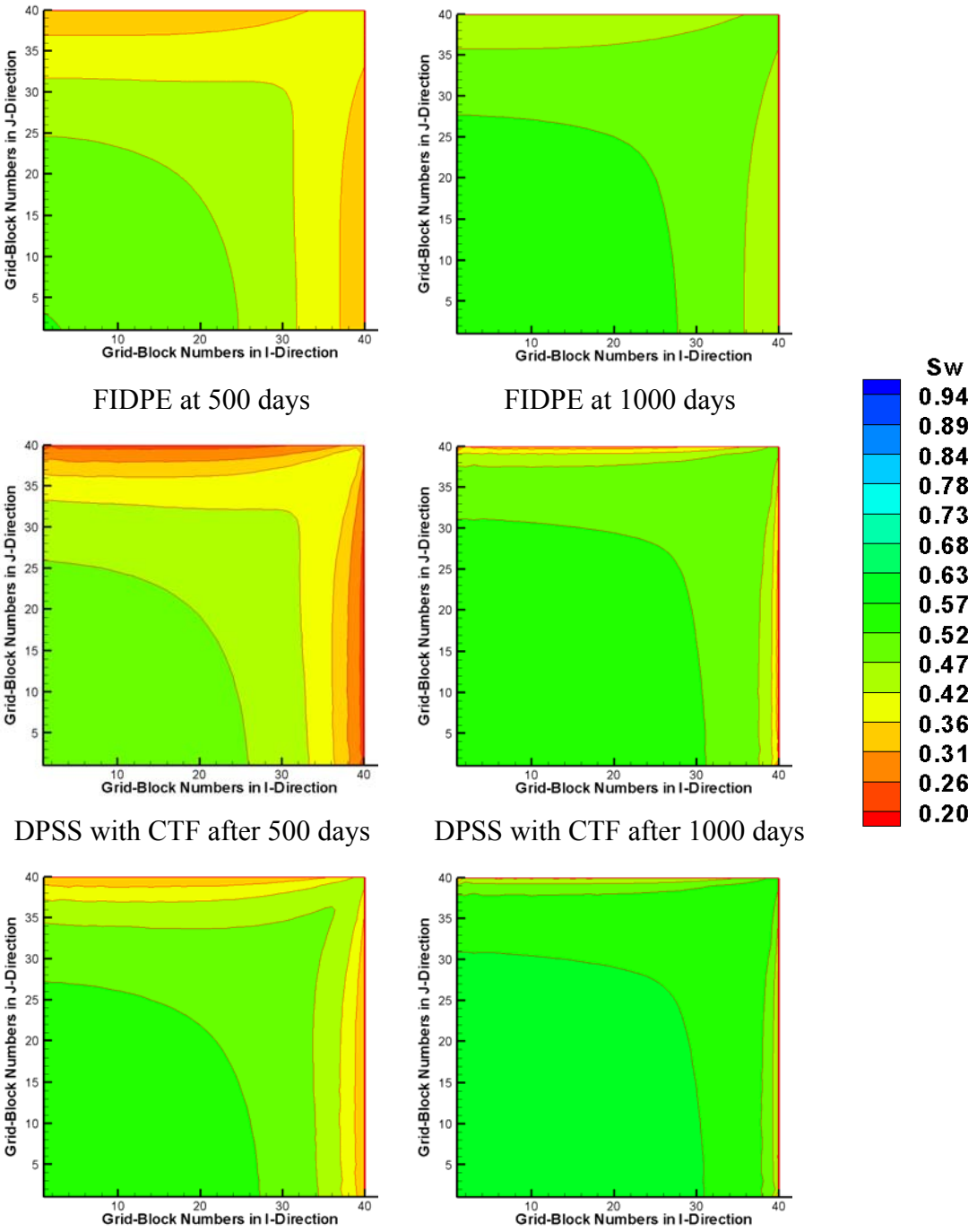

FIDPE at 500 days FIDPE at 1000 days

DPSS with CTF after 500 days DPSS with CTF after 1000 days

DPSS with ETF/ DTF at 500 days DPSS with ETF/ DTF at 1000 days

Figure 3.13-Comparison between DPSS and FIDPE in Terms of Matrix Water Saturation, Homogenous Case, Imbibition Process.

3.2.2 Heterogeneous Case: Quarter Five Spot Pattern

In this section, we extend our discussion to a quarter five spot heterogeneous case. The field parameters are similar to those in Table 3.5, except for the fracture permeability. The permeability field is similar to the one shown in Figure 3.1.The impact of running the DPSS with or without a transfer function is similar to the impact that we have seen in the homogenous case in the previous section. Figure 3.14 shows that the water saturation will advance facter when we run the DPSS without a transfer function. Figure 3.15 confirms the water saturation results and shows that the water cut is higher when we run the DPSS without a transfer function. The heterogeneity in this example can be realized by looking at the streamlines trajectories in Figure 3.16. The high contrast areas represent the high permeable zones where most of the streamlines pass through.

The water cut and recovery histories for DPSS with CTF and FIDPE are in a good agreement as shown in Figure 3.17. Fracture and matrix water saturation for both simulators shows good agreements as illustrated in Figure 3.18 and Figure 3.19. Figure 3.18 and Figure 3.19 show that FIDPE suffers from numerical smearing because we can not see sharp fronts in the saturation map. The sharp fronts in the DPSS saturation map are not due to our formulation but it is related to a fundamental difference between streamline simulation and finite difference simulation. In streamline simulation, viscous forces are solved by decoupling the 3D saturation equation in Cartesian coordinate into a series of 1D equation. This decoupling technique will allow solving the saturation equation in heterogeneous reservoir more efficiently and accurately with finer discretization along streamlines. Figure 3.20 shows fracture water saturation for DPSS and FIDPE without transfer function. Using DSPSS and FIDPE without transfer function are equivalent to using a single-porosity streamline simulation and a single-porosity ECLIPSE for fracture system only. Figure 3.20 indicate that the single-porosity ECLIPSE suffers from grid-block orientation and numerical smearing. It confirms that the differences between DPSS and FIDPE are not due to the implementation of the transfer function.

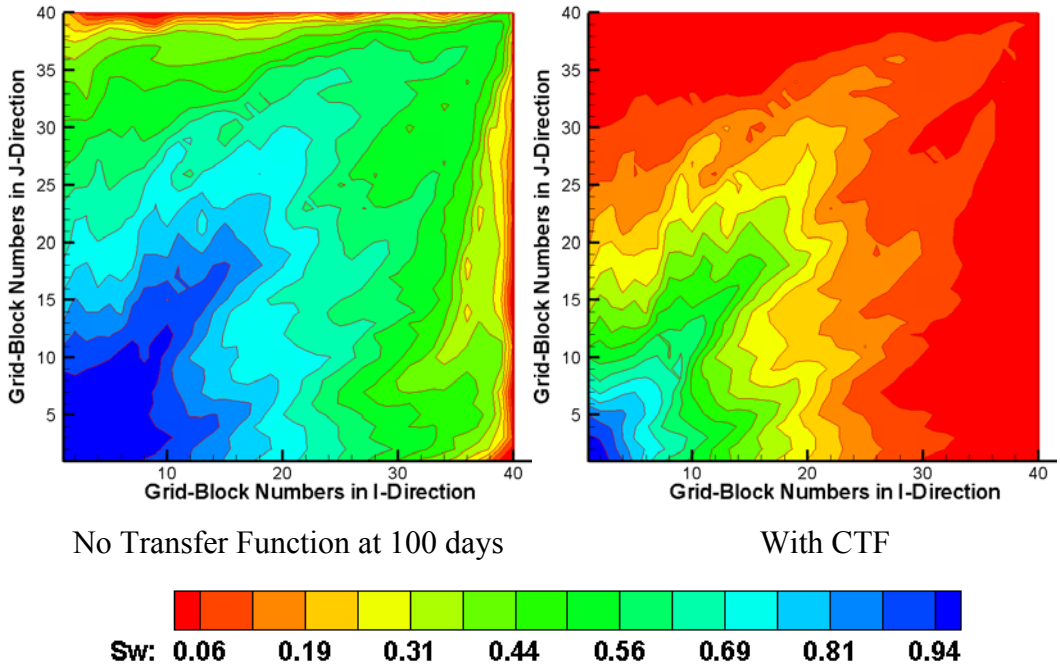

Figure 3.14-Comparison between DPSS with and without CTF in Terms of Fracture Water Saturation, Heterogeneous Case, Imbibition Process.

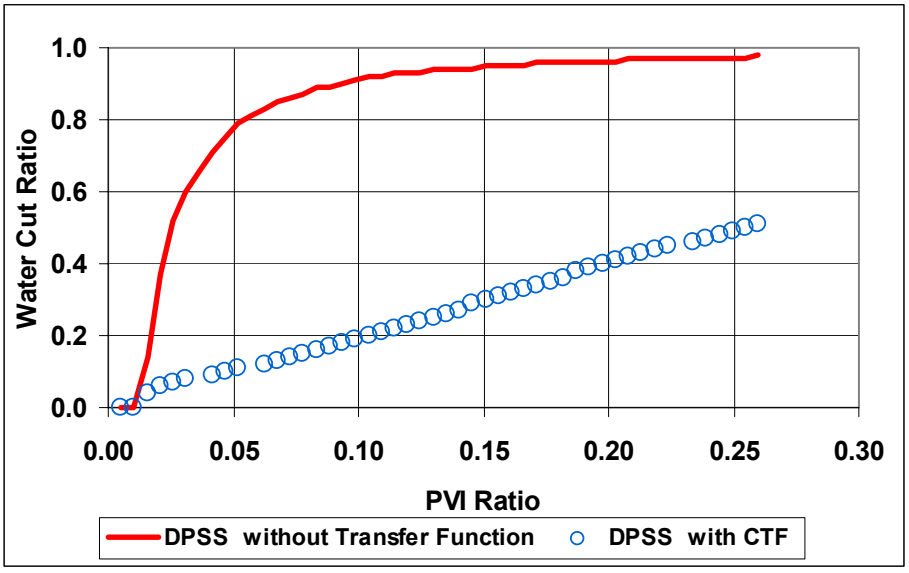

Figure 3.15-Comparison between DPSS with and without CTF in Terms of Water Cut History, Heterogeneous Case, Imbibition Process.

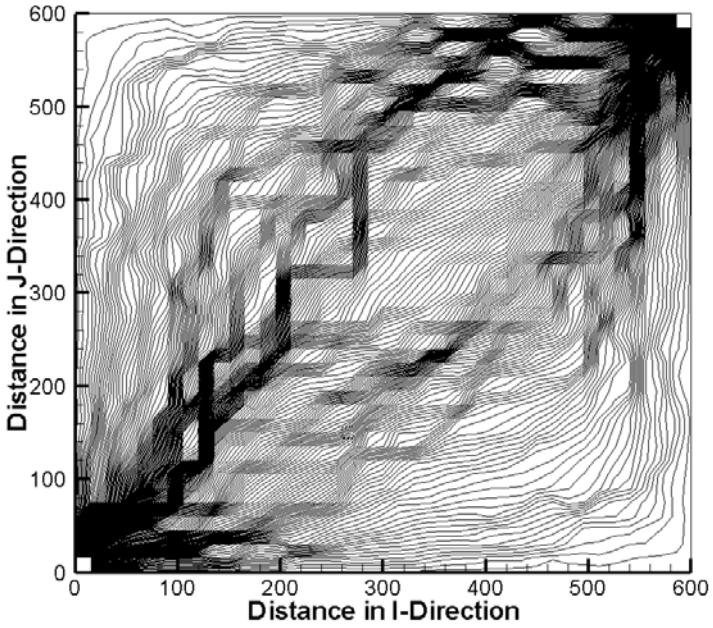

Figure 3.16-Streamlines in a Quarter Five Spot Pattern, Heterogenous Case, Imbibition Process.

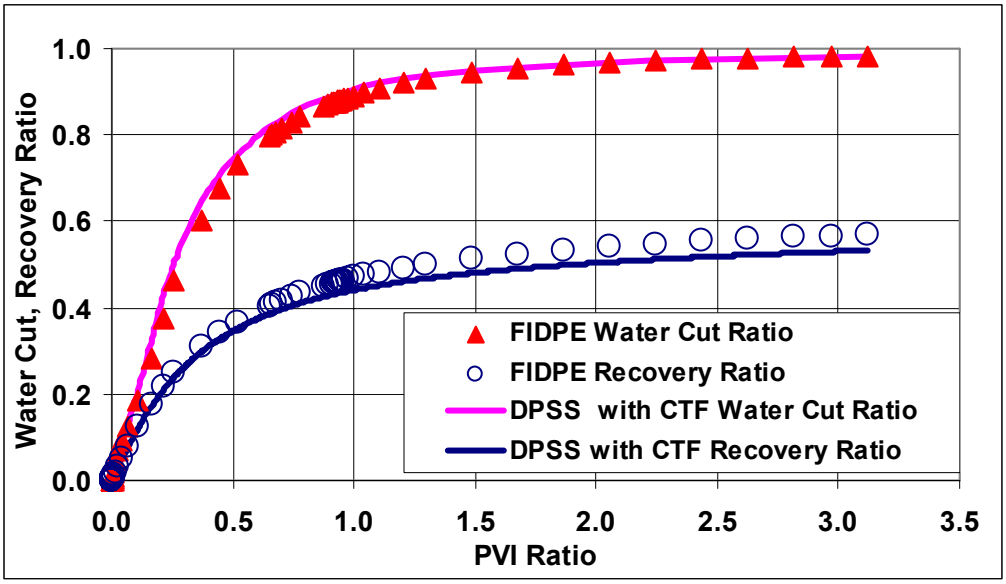

Figure 3.17-Comparison between FIDPE and DPSS with CTF in Terms of Water Cut and Recovery Ratios, Heterogeneous Case, Imbibition Process.

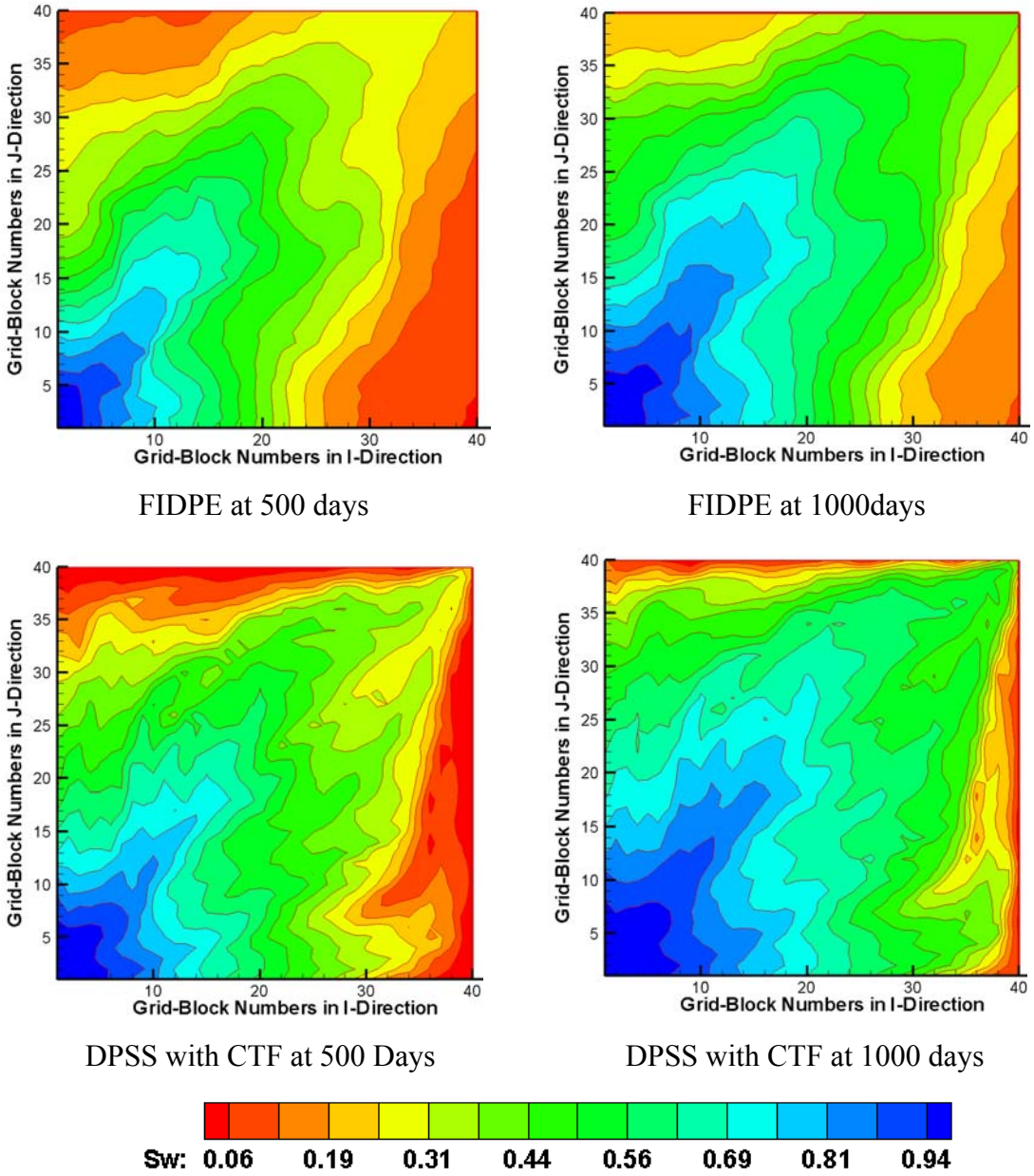

Figure 3.18-Comparison between DPSS and FIDPE in Terms of Fracture Water Saturation, Heterogeneous Case, Imbibition Process.

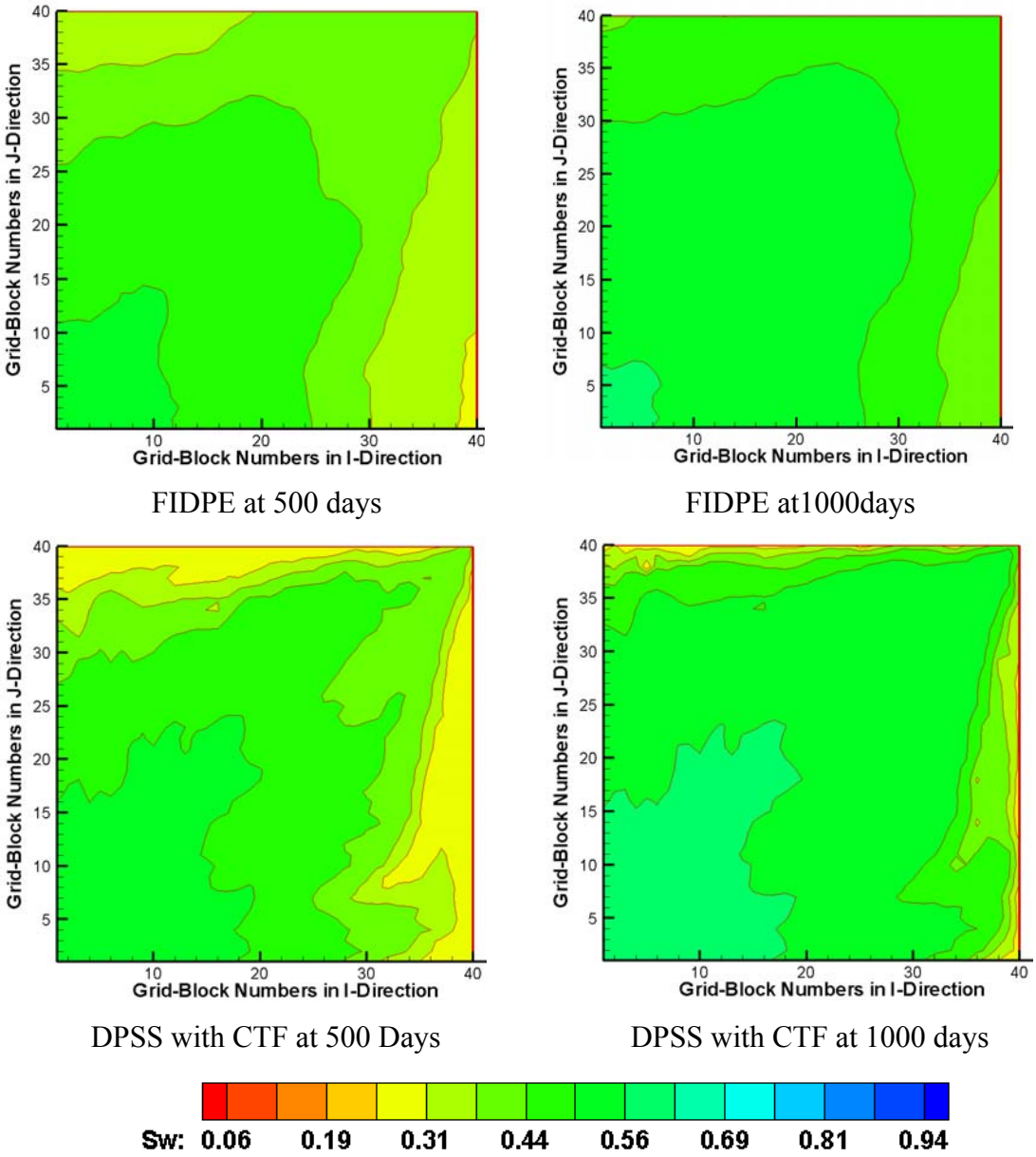

FIDPE at 500 days

FIDPE at1000days

DPSS with CTF at 500 Days

DPSS with CTF at 1000 days

Figure 3.19-Comparison between DPSS and FIDPE in Terms of Matrix Water Saturation, Homogenous Case, Imbibition Process.

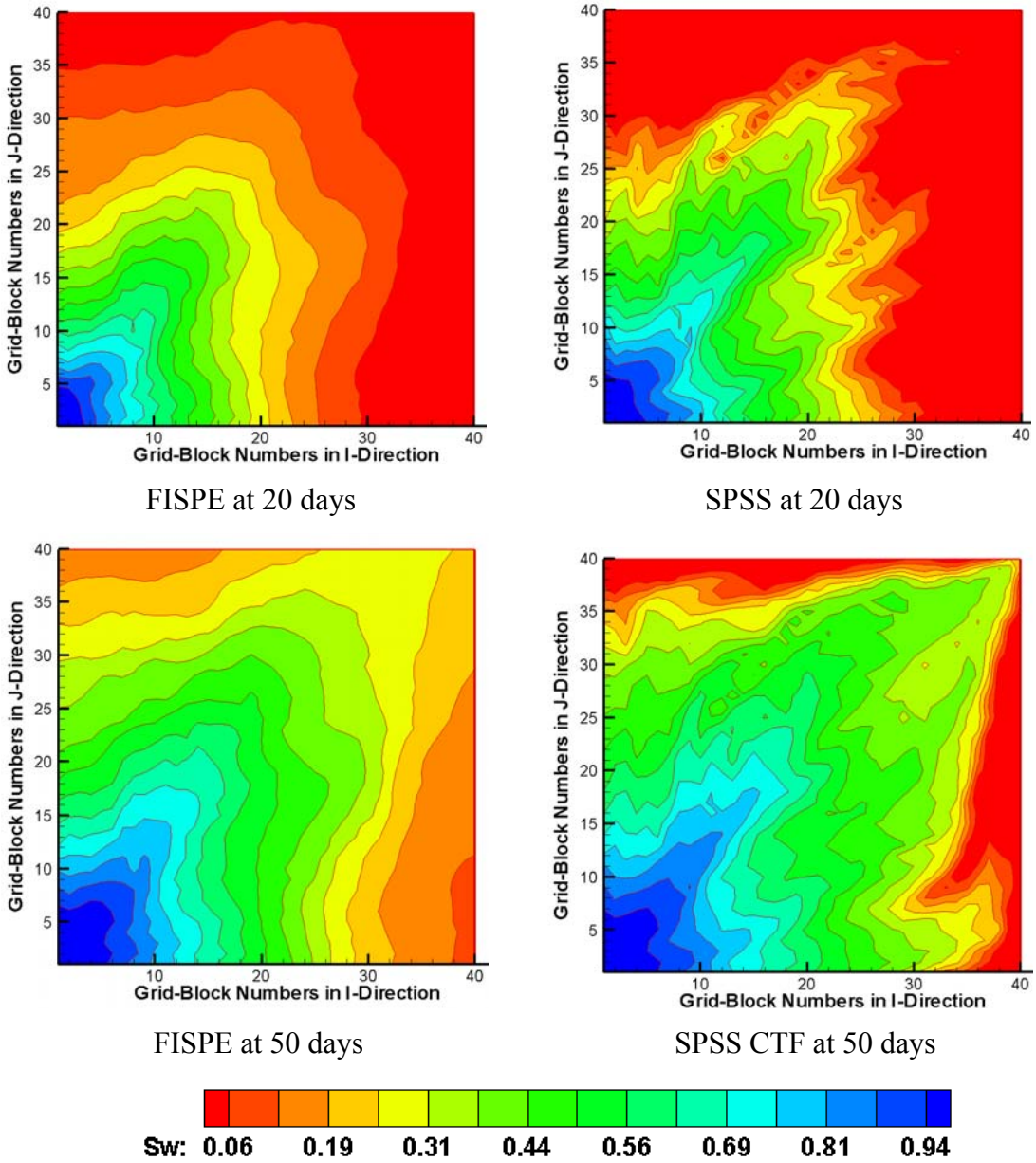

Figure 3.20-Comparison between SPSS and FISPE in Terms of Fracture Water Saturation, Heterogeneous Case, No Transfer Function.

3.3 Dual-Porosity Streamline (Gravity/Imbibitions Mechanism)

This section presents DPSS results when the Gravity/Imbibition process is the most dominant recovery mechanism. These results were compared to the results of FIDPE. The comparison is based on three examples: a homogenous quarter five-spot pattern, a homogenous nine-spot pattern, and a heterogeneous nine-spot pattern.

3.3.1 Homogenous Case: Quarter Five Spot Pattern

This example was designed to illustrate: (1) the impact of simulating naturally fractured reservoir with or without a transfer function, (2) the impact of using the CTF with or without gravity. Table 3.5 presents the field parameters, and Figure 3.3 and Figure 3.4 shows relative permeability and capillary pressure curves.

Figure 3.21 presents the water cut ratio for three scenarios using FIDPE. Those scenarios are: (1) running the simulator without a transfer function, (2) running the simulator with a transfer function describing the imbibition process only, and (3) running the simulator with a transfer function describing the gravity/imbibition process. The simulation run without transfer function shows the highest water cut response and the earliest breakthrough time. This result is logical because the interaction with the matrix-blocks was not considered. The simulation run with imbibition transfer function shows the lowest water cut response, but this is not necessarily true for all field. This field case shows that the gravity will tend to reduce the recovery from the matrix.

Figure 3.22 shows that the DPSS simulator predicts the same behavior as FIDPE. In Figure 3.23, we compare both simulators in terms of water cut response. They have almost identical results.

Table 3.5-Quarter Five Spot Pattern Parameters, Homogenous Case, Gravity/Imbibition Process.

Parameters	Values
Dimension In I-Direction, ft	2000
Dimension In J-Direction, ft	2000
Matrix-Block Thickness, l_z, ft	30 ft
Reservoir Grid	40 × 40×1
Injection Rates, STB/Day	400
Production Rate, STB/Day	400
k_f, md	500
k_m, md	1
F_s, ft^2	0.12
ϕ_f	0.05
ϕ_m	0.19
μ_w, cp	0.5
μ_o, cp	2
ρ_w, psi/ft	0.44
ρ_o, psi/ft	0.3611
P_i, psi	4000

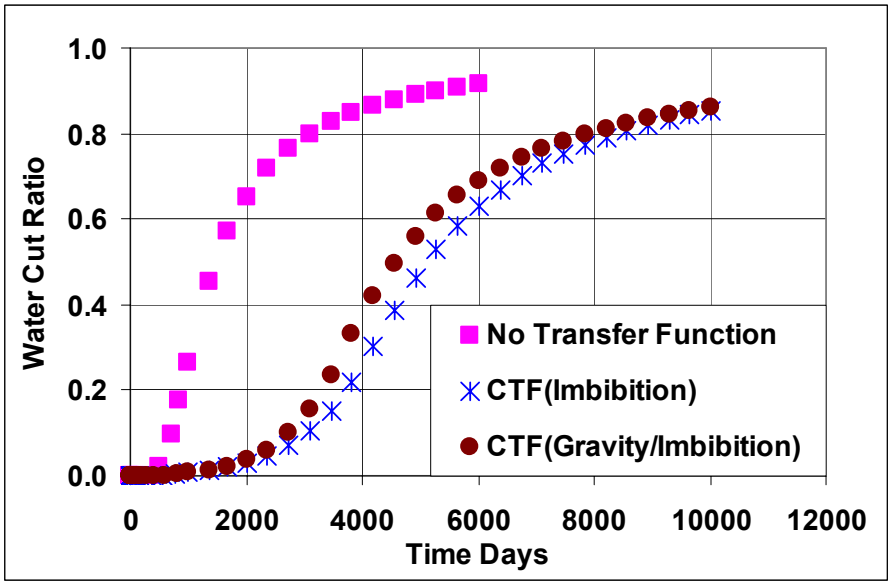

Figure 3.21-FIDPE Water Cut History, Quarter Five Spot Pattern, Gravity/Imbibition Process.

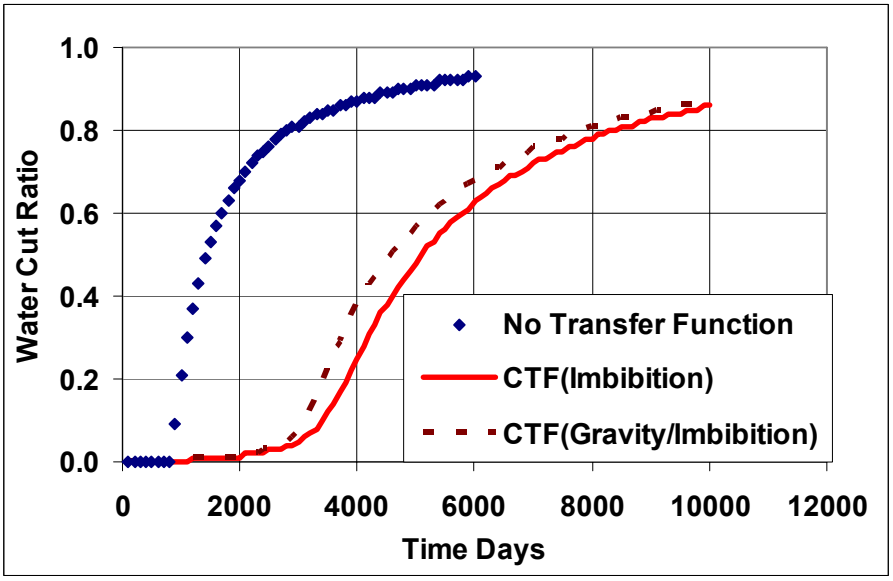

Figure 3.22-DPSS with CTF Water Cut History, Quarter Five Spot Pattern, Gravity/Imbibition Process.

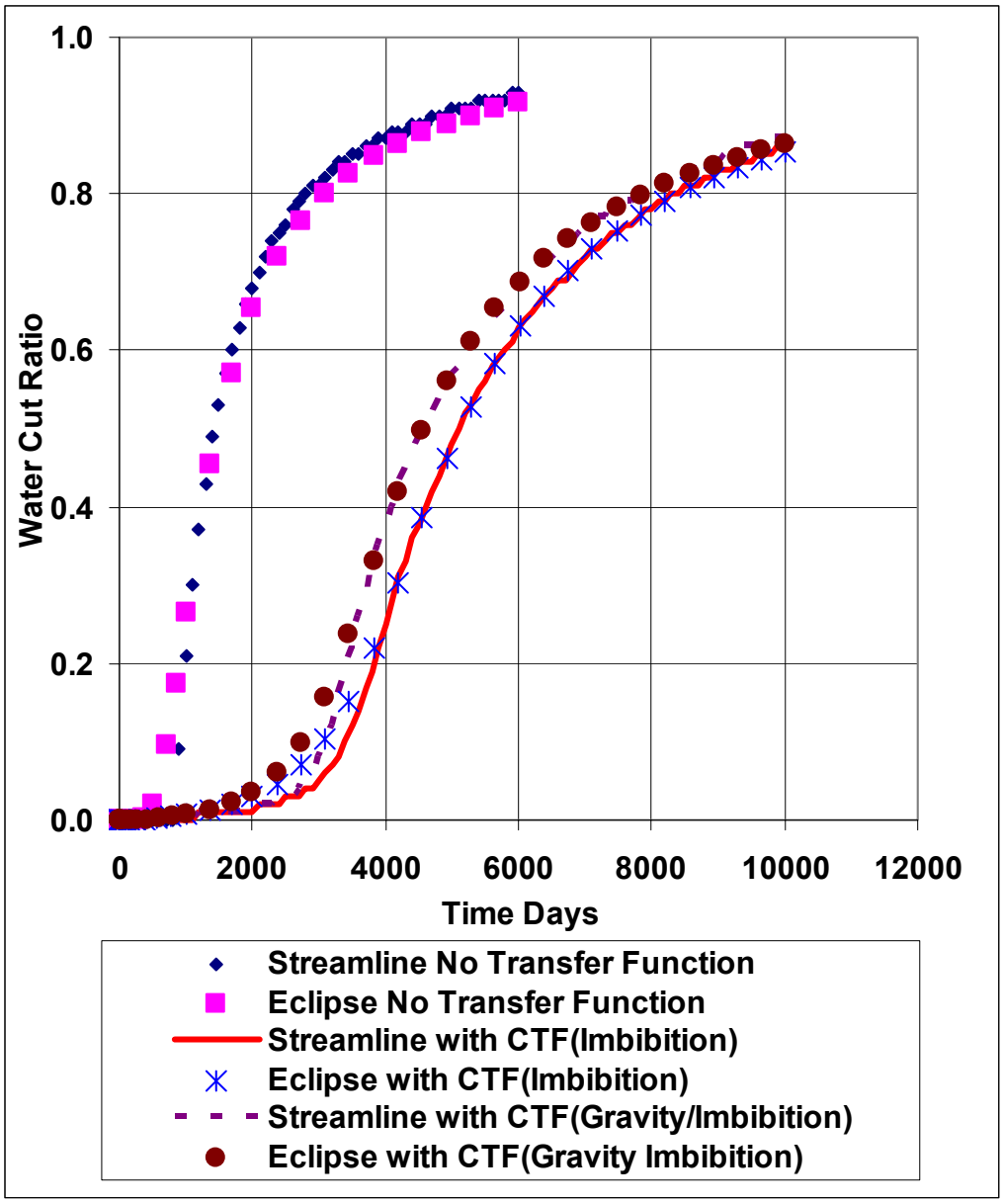

Figure 3.23-Comparison between DPSS with CTF and FIDPE in Terms of Water Cut History, Quarter Five Spot Pattern, Gravity/Imbibition Process.

3.3.2 Homogenous Case: Nine Spot Pattern

In this section, we present a comparison between DPSS with CTF and FIDPE for a nine spot field example. Table 3.6 presents the field parameters and Figure 3.3 and Figure 3.4 shows the relative permeability curves used in this example.

Figure 3.24 shows the streamlines in this example. Figure 3.25 shows a comparison between DPSS with CTF and FIDPE in terms of water cut and recovery ratios. The results indicate an excellent agreement between both simulators. For individual well, the water cut and recovery responses for both simulators are in good agreement as shown in Figure 3.26. Fracture and matrix water saturation for both simulators are in a good agreement as shown in Figure 3.27. Figure 3.27 shows that FIDPE suffers from grid orientation because the propagation of saturation around the injector is not exactly circular. In the finite-difference simulator, saturation propagates along the vertical and horizontal direction faster than the diagonal directions. In streamline simulation, saturation propagates along the streamlines which are minimally affected grid orientations as shown in Figure 3.24.

Table 3.6-Nine Spot Pattern Parameters, Homogenous Case, Gravity/Imbibition Process.

Parameters	Values
Dimension In I-Direction, ft	2000
Dimension In J-Direction, ft	2000
Thickness, ft	30 ft
Matrix-Block Thickness, l_z, ft	30 ft
Reservoir Grid	41 × 41×1
Injection Rates, STB/Day	800
Production Rate for each Well, STB/Day	100
k_f, md	500
k_m, md	1
F_s, ft^2	0.0844
ϕ_f	0.05
ϕ_m	0.2
μ_w, cp	0.5
μ_o, cp	2
ρ_w, psi/ft	0.44
ρ_o, psi/ft	0.3611
P_i, psi	4000

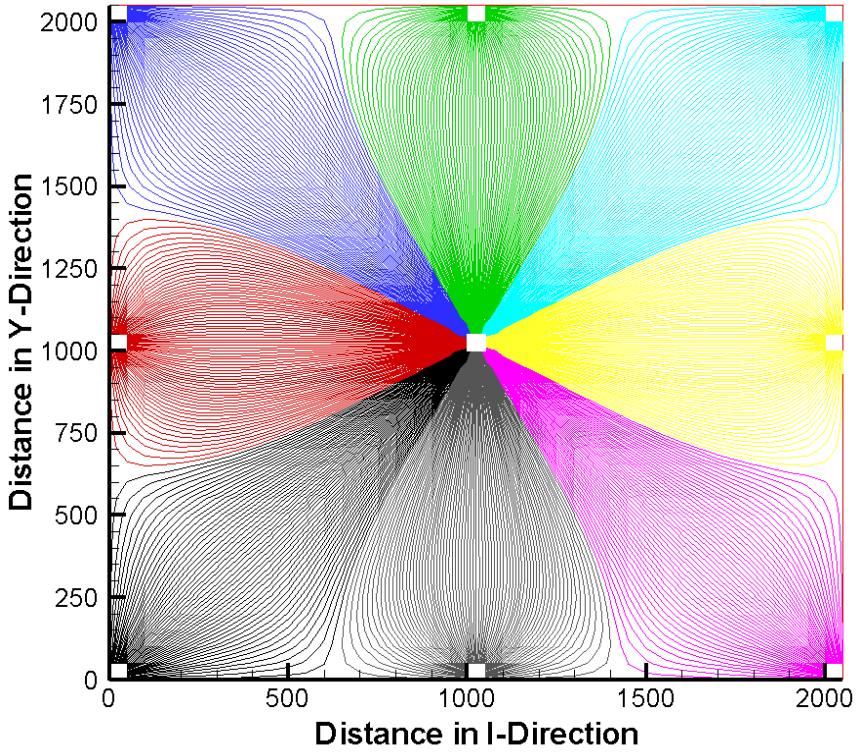

Figure 3.24-Streamlines in a Nine Spot Pattern, Homogenous Case, Gravity/Imbibition Process.

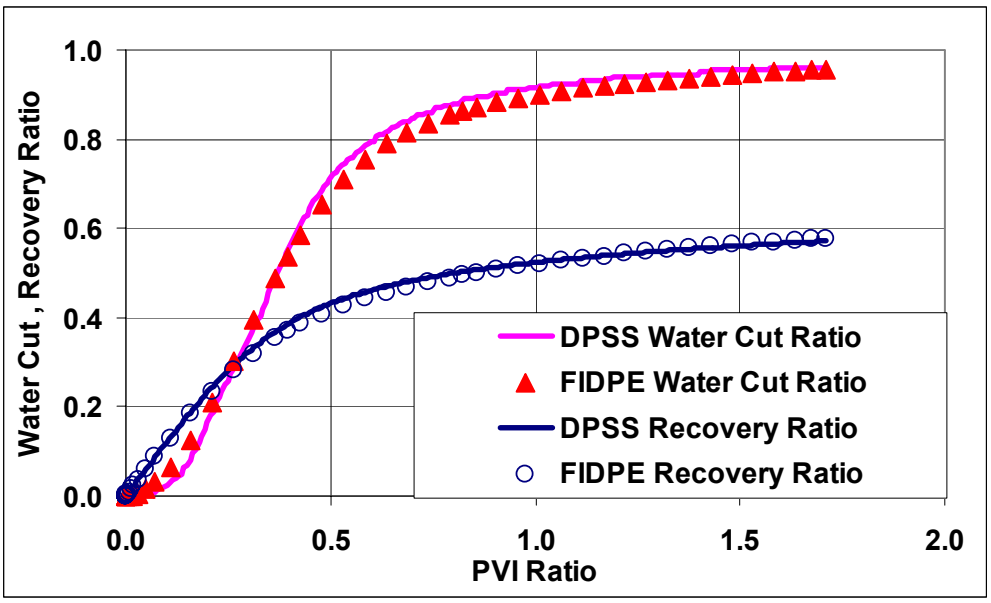

Figure 3.25-Comparison between FIDPE and DPSS with CTF in Terms of Field Water Cut and Recovery Histories, Homogenous Nine Spot Case, Gravity/Imbibition Process.

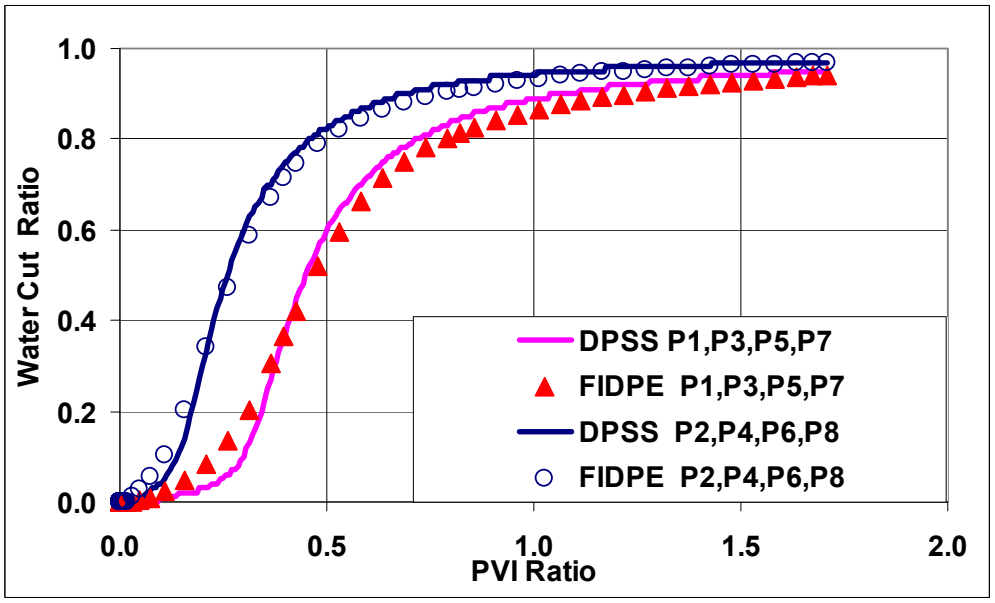

Figure 3.26-Comparison between FIDPE and DPSS with CTF in Terms of Water Cut History for Each Well , Homogenous Nine Spot Case, Gravity/Imbibition Process.

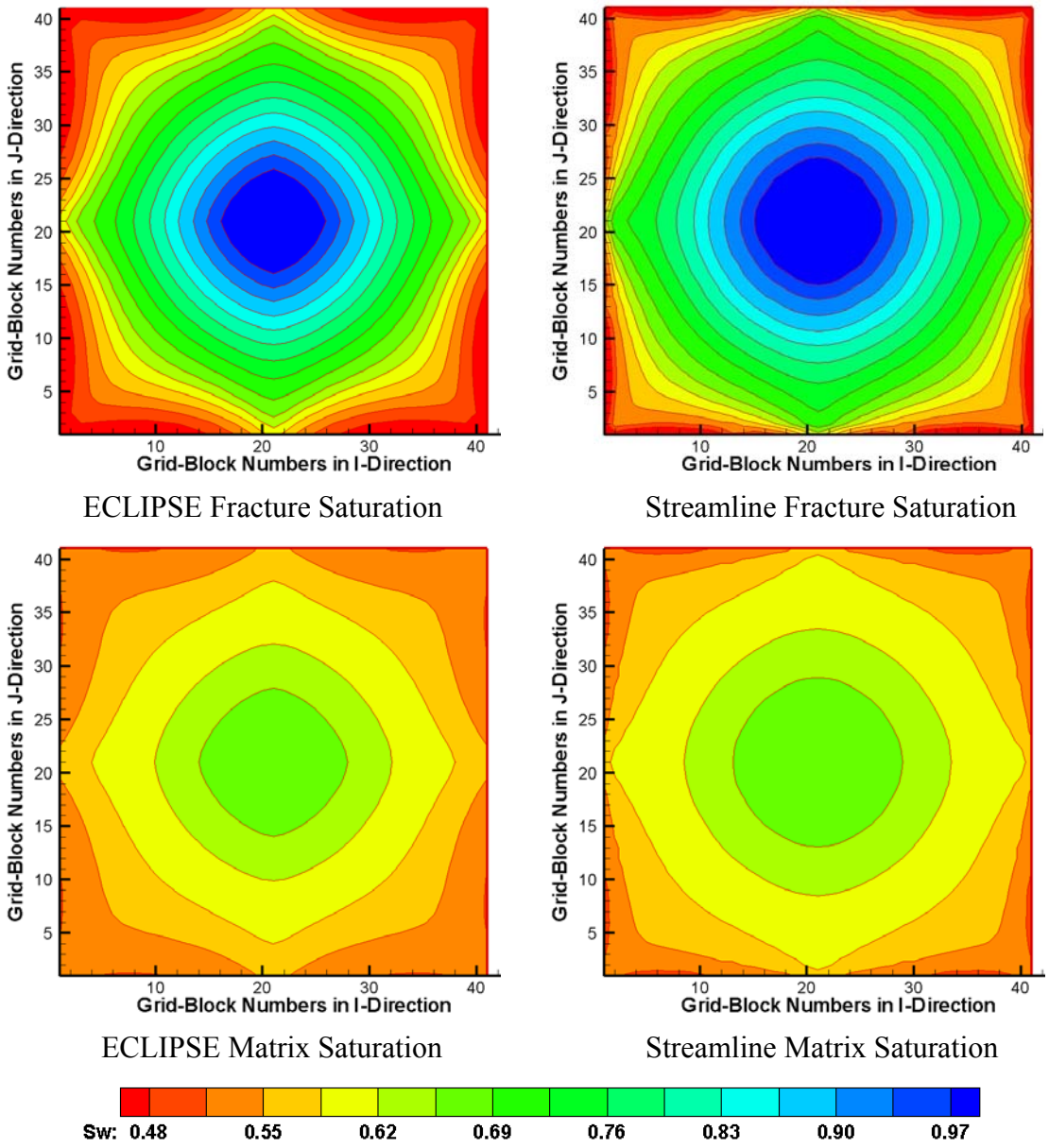

Figure 3.27-Comparison between DPSS and FIDPE in Terms of Fracture Water Saturation, Heterogeneous Case, Gravity/Imbibition Process.

3.3.3 Heterogeneous Case: Nine Spot Pattern

In this section, we extend the discussion in the previous section and present and present a comparison between DPSS with CTF and FIDPE for a heterogeneous nine spot example. The field parameters are similar to those in the homogenous nine spot pattern except for the fracture permeability. The permeability field is similar to the 2D permeability map shown in Figure 3.1.

Figure 3.28 shows how streamlines reflect the heterogeneity of this field. The water cut and recovery histories for DPSS with CTF and FIDPE are almost identical as shown in Figure 3.29. For individual wells, the water cut and recovery ratio for both simulators are in good agreements as shown in Figure 3.30. Fracture and matrix water saturation for both simulators shows a good match as illustrated in Figure 3.31. Figure 3.31 show that for the same grid size, FIDPE suffers from grid orientations and numerical smearing because we can not see sharp fronts in the saturation map.

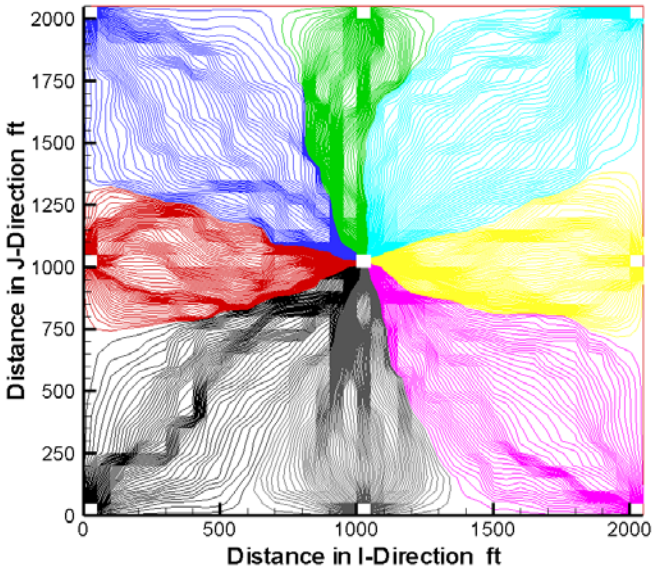

Figure 3.28-Streamlines in a Nine Spot Pattern, Heterogeneous Nine Spot Case, Gravity/Imbibition Process.

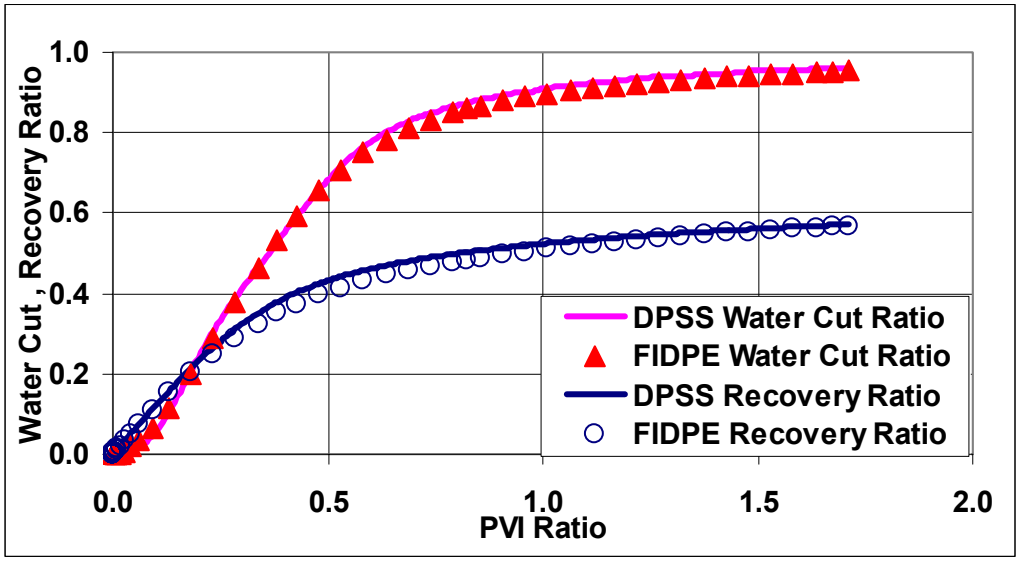

Figure 3.29-Comparison between FIDPE and DPSS with CTF in Terms of Field Water Cut and Recovery Ratios, Heterogeneous Nine Spot Case, Gravity/Imbibition Process.

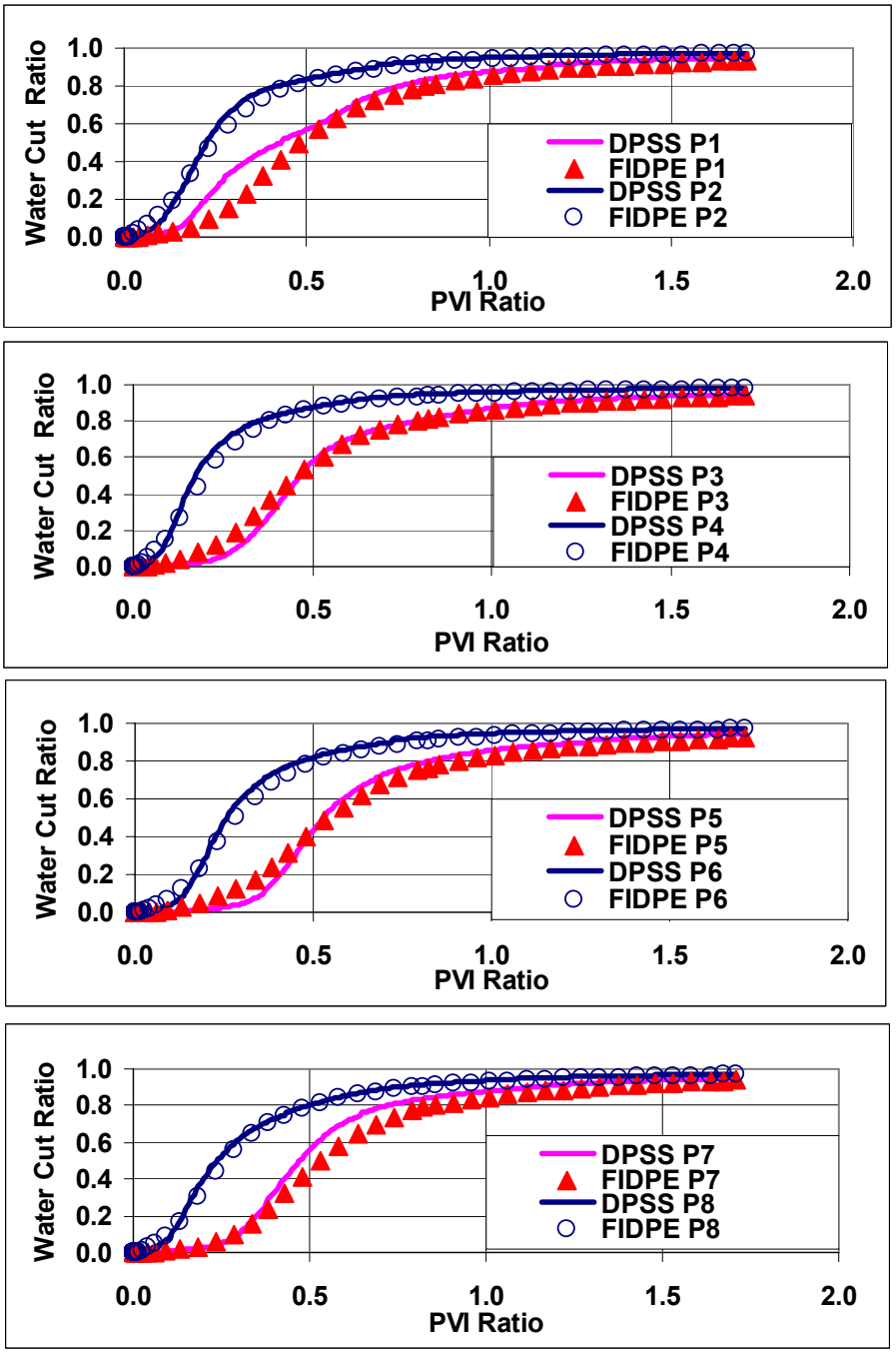

Figure 3.30-Comparison between FIDPE and DPSS with CTF in Terms of Well Water Cut Ratio, Heterogeneous Nine Spot Case, Gravity/Imbibition Process.

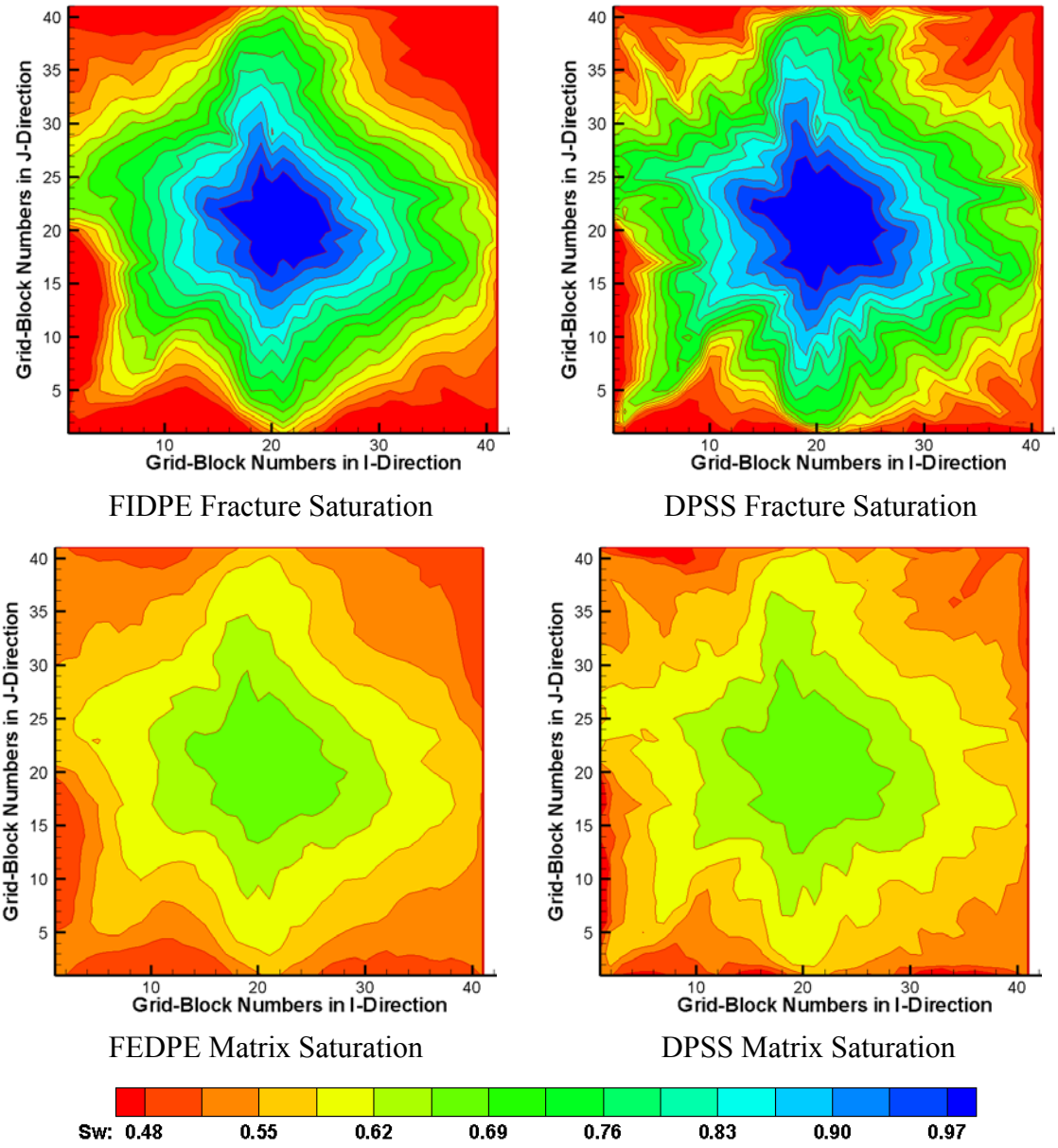

Figure 3.31-Comparison between DPSS and FIDPE in Terms of Fracture Water Saturation after 6000 Days, Heterogeneous Nine Spot Case, Gravity/Imbibition Process.

3.4 CPU Time and Numerical Smearing

In this section, we present a comparison between DPSS, FIDPE and IMPESDPE in terms of CPU time and numerical smearing. Conventional single-porosity finite-difference techniques suffer mainly from numerical smearing and computational burden for large and heterogeneous geological models.

Although the IMPES (Implicit Pressure Explicit Saturation) method has less numerical smearing effects than the fully implicit method in the single-porosity simulation, it suffers from the limitation in time-step size based on Courant-Friedrichs-Lewy (CFL) limit. The maximum time-step size gets shorter as the number of cells increases for a given model. For large models, the CPU time will be large and it is not practically efficient to use the IMPES method. The fully implicit method can offer stability without any limitation on the time-step but it suffers from numerical smearing.

We demonstrate that the dual-porosity finite-difference simulation suffers from the same drawbacks as the single-porosity system. We will show that the streamline approach will offer a promising technique to overcome those drawbacks.

In terms of CPU time, we performed multiple runs on a 3D homogenous case with different number of grids using FIDPE, IMPESDPE, and DPSS. For FIDPE, we used the default tuning parameter in ECLIPSE for fully implicit method. Also, we used the default tuning parameter for IMPESDPE except for the allowable maximum saturation and pressure change during the time step. We used 0.2 maximum saturation change and 400 psi maximum pressure change in IMPES method. In DPSS, we choose the number of nodes along each streamline to be equal to the number of grids that the streamline passes through. The time-step to solve the saturation equation numerically is set to $\Delta t = 0.9\Delta\tau$. Table 3.7 shows the parameters used to perform this task. Figure 3.3 and Figure 3.4 shows the relative permeability and capillary pressure curves used in this example.

Table 3.7-Quarter Five Spot Pattern Parameters, Homogenous Case, CPU Time.

Parameters	Values
Dimension In I-Direction, ft	1000
Dimension In J-Direction, ft	1000
Thickness, ft	100 ft
Injection Rates, STB/Day	1000
Production Rate, STB/Day	1000
k_f, md	500
k_m, md	1
F_s, ft^2	0.05
ϕ_f	0.05
ϕ_m	0.25
μ_w, cp	0.5
μ_o, cp	2
ρ_w, psi/ft	0.44
ρ_o, psi/ft	0.3611
P_i, psi	4000

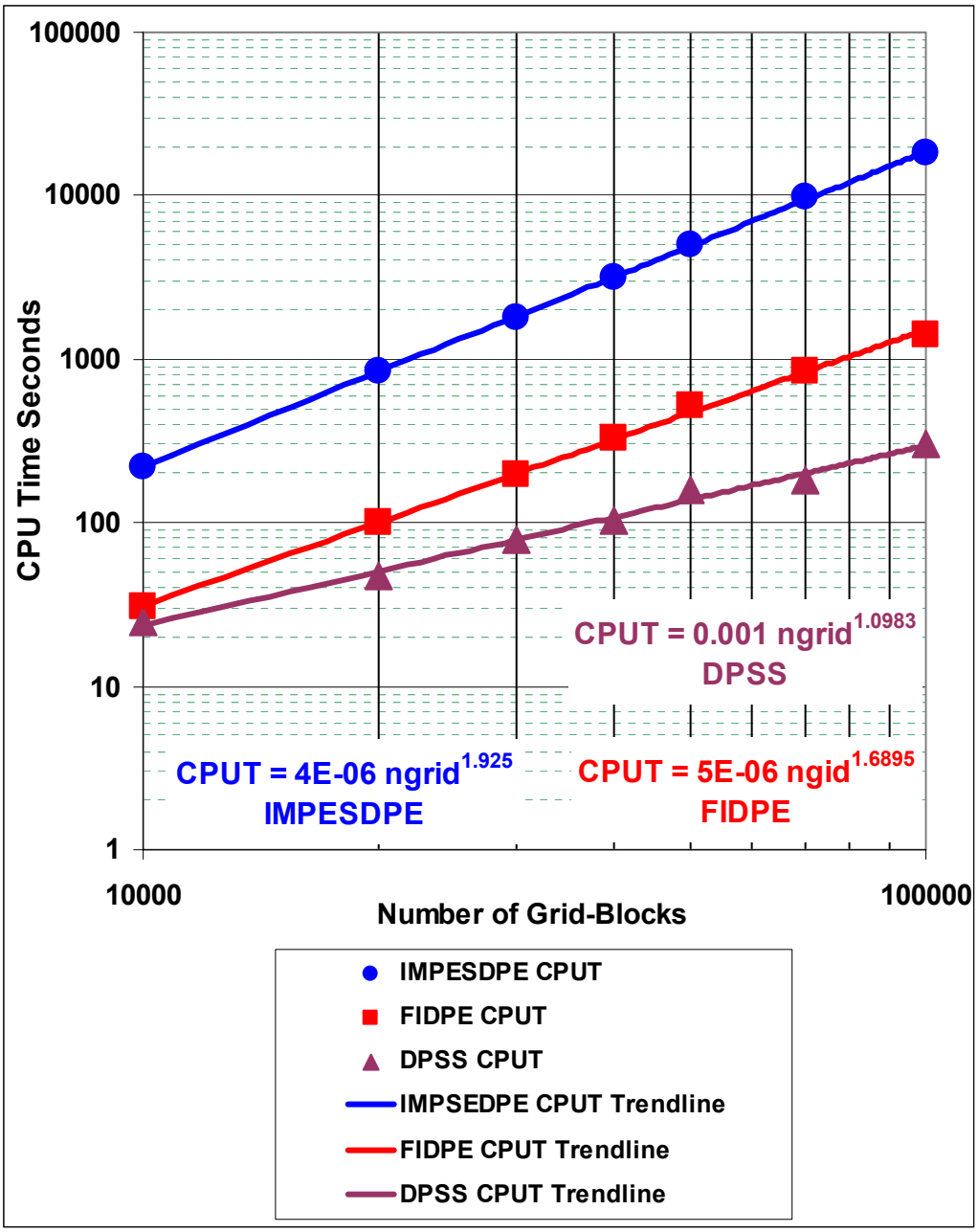

Figure 3.32-CPU Time Comparison between FIDPE, IMPESDPE, and DPSS.

Figure 3.32 shows CPU time comparison between FIDPE, IMPESDPE, and DPSS. The CPU time for IMPESDPE has quadratic relationship with the grid-block numbers. This indicates that using IMPESDPE for large models is not computationally efficient. The FIDPE shows some improvement in CPU time with a scaling exponent of 1.69 compared to 2 for IMPES. On the other, the DPSS CPU time increases linearly as the number of grid-block increases. The results illustrate that the DPSS is ideal for large simulation models.

In terms of reducing the numerical smearing in heterogeneous models, DPSS outperform the FIDPE as shown in Figure 3.18, Figure 3.19, and Figure 3.31. The finite-difference results can be improved by decreasing the grid-block size but at a considerable computational expense. Using the IMPESDPE instead of FIDPE will not improve much as shown in Figure 3.33. Figure 3.33 presents a comparison between FIDPE and IMPESDPE in terms of fracture and matrix water saturation. The field example used to perform this comparison is the heterogeneous nine spot pattern which has been used to compare the DPSS and the FIDPE in Figure 3.31. No significant differences can be seen in the saturation profiles.

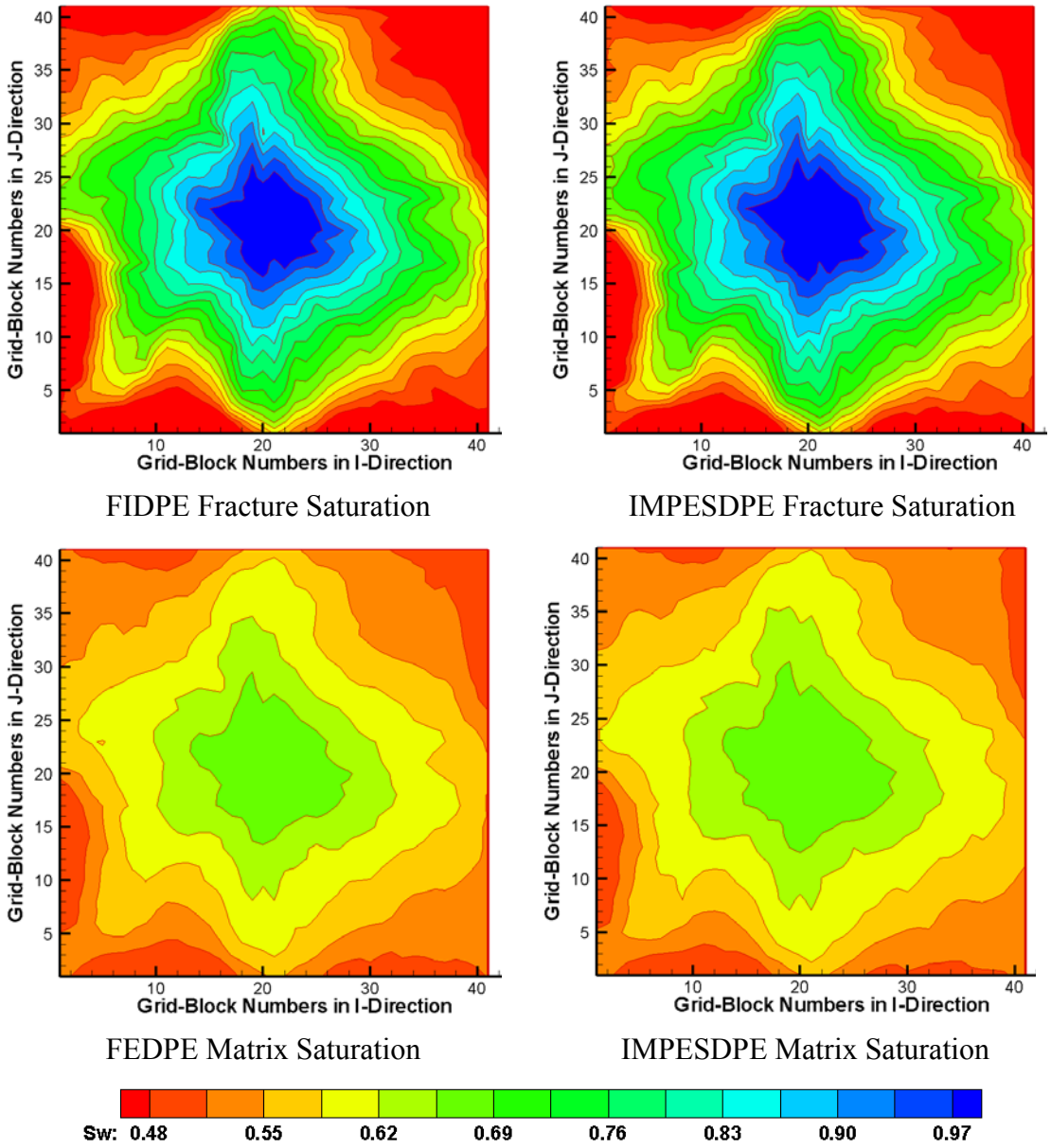

Figure 3.33-Comparison between FIDPE and IMPESDPE in Terms of Fracture and Water Saturation after 6000 Days, Heterogeneous Nine Spot Case, Gravity/Imbibition.

CHAPTER IV
SUMMARY AND RECOMMENDATIONS

This chapter summarizes the thesis with major findings and recommendations.

4.1 Major Findings

The main focus of our work has been to generalize the streamline-based simulation to describe fluid transport in naturally fractured reservoir. The previous formulation was limited only for single-porosity systems. The major findings of our study are:

- The fluid flow and transport equations needed to simulate fluid dynamics in dual-porosity single-permeability system are discussed

- The water saturation equation in fractured systems was derived in terms of streamline time-of-flight and has been decupled from the pressure equation assuming that the amount of oil expelled from the matrix-blocks is equal to the amount of water imbibed into the matrix-blocks.

- A transfer function was added to the saturation equation as a source term. This source term takes care of fluid exchange between matrix-block and fracture system.

- The Transfer function doesn't appear in the pressure equation and then doesn't affect streamlines trajectories.

- Three different types of transfer functions have been studied: conventional transfer function (CTF), empirical transfer function (ETF), and diffusion transfer function (DTF). All transfer functions depend only on saturation and mainly

describe the imbibition process. We showed how to account for gravity/imbibition process in the CTF.

- Numerical solution for the saturation equation with all types of transfer function has been derived.

- The numerical solution of the saturation equation with ETF and DTF requires discretization of a convolution term. So, we derived an analytical solution in terms of TOF to validate the numerical solution. The comparison of both solutions showed an excellent match.

- Although our analytical solution was derived using similar procedures done by Kazemi *et al.*[32], it is not limited only for 1D problems because of the time of flight formulation.

- The dual-porosity streamlines simulator (DPSS) with CTF has been compared to the fully implicit dual porosity ECLIPSE (FIDPE) when the imbibition proceses is the dominant force to derive oil form the matrix-block. The comparison was based on quarter five spot homogenous and heterogeneous cases. Both simulators showed comparable results in terms of water cut and recovery ratios. In terms of water saturation distribution, they showed comparable results but DPSS results were more accurate in reflecting the heterogeneity in the heterogeneous case.

- On the other hand, the DPSS with ETF and DTF showed that the water saturation advances faster in fracture and matrix system than the water saturation obtained from the FIDPE and the DPSS with CTF. The reason behind this difference was not investigated further. The main scope of this study was to implement different transfer functions in the streamline formulation and not to investigate their relative accuracy.

- The DPSS with CTF has been compared to the FIDPE when the gravity/imbibition process is the dominant force to recover oil from the matrix-block. The comparison was based on three different cases: a quarter five spot homogenous case, a nine spot homogenous case, and a nine spot homogenous case. The match between the results was excellent. The comparison in terms of water saturation distribution showed that the DPSS predict the saturation evolution more accurately.

- The DPSS outperform FIDPE and IMPES dual-prosity ECLIPSE (IMPESDPE) in terms of CPU time and minimizing the numerical smearing and grid-block orientation effects. The superiority of DPSS is due to decoupling the three dimensional saturation equation into a series of 1D equations which can be solved with higher accuracy.

4.2 Recommendations

Due to the time constraints, we couldn't investigate the implementation of DPSS in a real field example, extend our formulation to describe the fluid transport in dual-porosity dual-permeability system, use matrix sub-griding technique to describe the interaction between fracture system and matrix-blocks, and test the stability of the numerical solution of the saturation equation.

In dual-porosity dual-permeability system, both matrix and fracture system contribute to flow at the wellbore. In this case there is a pressure gradient in both systems and streamlines have to be traced in both systems. Tracing the streamlines is easy because the pressure field can be generated in a similar way as in the finite-difference methods. The assumptions that we have made in dual-porosity system might not be applicable in dual-porosity dual-permeability system. We have assumed that the amount of water imbibed into the matrix system is equal to the amount of oil expelled from the matrix

system. The matix/fracutre transfer function will not depend only on saturation as in the dual-porosity single-permeability system, but also on the phase pressure. The main concern is that the phase pressures in fracture and matrix system can change drastically, requiring a lot of pressure updates. This might limit the application of streamline simulation in dual-porosity dual-permeability systems.

Sub-gridding the matrix-block into many sub-domains will enhance the accuracy of the transfer function. It can describe the transient behavior and gravity segregation in the matrix-block efficiently. In our formulation, we lumped the matrix-blocks into one source term connected to the fracture system. This type of modeling is efficient especially for models where matrix-blocks are large and wells are producing at low rates. In finite-difference methods, the technique requires pressure and saturation not only in the fracture system, but also in each matrix-block sub-domains. Each sub-domain can have its own petrophysical properties and shape factor. The key point to make this technique suit streamline simulation is to eliminate the dependency of the transfer function on phase pressure in fracture system and matrix sub-domains. One way to do that is to assume that the amount of water imbibed into each sub-domain equals to the amount of oil expelled from each sub-domain. Also, the total amount of water imbibed from the fracture system is equal to the total amount of oil expelled to the fracture system. So far, we haven't validated this approach.

The explicit scheme used to solve the saturation equation in single porosity streamline simulation is numerically stable if the convective time-step, Δt, is less than $\Delta \tau$. This stability can't be guaranteed in dual-porosity streamline simulation because the saturation equation has an additional term, the transfer function. If we consider the saturation equation with CTF, there is a great chance that we have stability problem if the volumetric fluid transfer between the matrix and the fracture systems is large during the convective time-step, Δt. This can happen for large values for the shape factor and the matrix permeability. The easiest solution for this problem is to decrease Δt whenever

we have a stability problem. This solution sounds easy, but it might be at a considerable computational expense. The most efficient method to overcome this problem is to solve the saturation equation along the streamlines fully implicitly. The fully implicit scheme for the saturation equation in the dual-porosity streamline simulation will guarantee unconditional stability and allow large Δt.

NOMENCLATURE

a = empirical constants, dimensionless

D = depth, L

$D(S)$ = Capillary diffusion coefficient, ML^3T^{-2}

f = fractional flow, fraction

F_s = shape factor, L^{-2}

g = gravity acceleration

k = permeability, L^2

k_r = relative permeability, dimensionless

l = matrix length, L

P = pressure, $ML^{-1}T^{-2}$

P_c = capillary pressure, $ML^{-1}T^{-2}$

P_{gh} = pressure due to a gravity head in fracture system, $ML^{-1}T^{-2}$

q = source term, L^3T^{-1}

Q_∞ = ultimate oil. recovery, L^3

Q = cumulative oil. recovery, L^3

S = saturation, fraction

S_{orm} = matrix residual oil saturation, dimensionless

S_{wnm} = normalized water saturation in matrix, dimensionless

t = time, T

u = velocity, LT^{-1}

GREEK LETTERS

α = rate constant, T^{-1}

ϕ = porosity, fraction

ε = Integration variable

θ = contact angle, degree

λ = mobility, $M^{-1}LT$

μ = viscosity, $ML^{-1}T^{-1}$

ξ = constant

ρ = density, ML^{-3}

σ = interfacial tension, MT^{-2}

τ = time of flight, T

ω = rate constant, T^{-1}

SUBSCRIPTS

D = dimensionless

f = fracture

i = index

m = matrix

n = index

o = oil

w = water

x = x-direction

y = y-direction

z = z-direction

OPERATORS

∂ = partial derivative

∇ = gradient

Δ = finite difference

$\sum$ = summation

$\int$ = integration

ABBREVIATIONS

CTF	= conventional transfer function
DPSS	= dual-porosity streamline simulator
DTF	= diffusive transfer function
ETF	= empirical transfer function
FIDPE	= fully implicit dual-porosity ECLIPSE
FISPE	= fully implicit single-porosity ECLIPSE
IMPES	= implicit pressure explicit saturation
IMPESDPE	= IMPES dual-porosity ECLIPSE
SPSS	= single-porosity streamline simulator
TOF	= time of flight

REFERENCES

1. Batycky, R.P.: "A Three-Dimensional Two-Phase Field Scale Streamline Simulator," PhD dissertation, Stanford U., Stanford, CA (1997).
2. Batycky, R.P., Blunt, M.J., and Thiele, M.R.: "A 3D Field Scale Streamline-Based Reservoir Simulator," *SPERE* (November 1997) 246.
3. Peddibholta, S., Cubillos, H., Datta-Gupta, A., and Wu, C.H.: "Rapid Simulation of Multiphase Flow Through Fine-Scale Geostatistical Realizations Using a New, 3-D, Streamline Model : A Field Example," paper SPE 36008 presented at 1996 Petroleum Computer Conference , Dallas, TX, 2-5 June.
4. Choudhary, M.K.: "Reservoir Management Using Streamline Simulation," MS thesis, Texas A&M U., College Station, TX (2000).
5. King, M.J. and Datt-Gupta, A.: "Streamline Simulation: A Current Perspective," *In Situ* (1998) **22**, No.1, 91.
6. Vasco, D.W., Yoon, S., and Datta-Gupta, A.: "Integrating Dynamic Data Into High-Resolution Reservoir Models Using Streamline-Based Analytic Sensitivity Coefficients," paper SPE 49002 presented at the 1998 SPE Annual Technical Conference and Exhibition, New Orleans, LA, 27-30 September.
7. Muskat, M.: *Flow of Homogenous Fluids*, International Human Resources Development Corporation, Boston, MA (1973).
8. Fay, C.H. and Prats. M.: "The Application of Numerical Methods to Cycling and Flooding Problems," Proceedings of the 3rd World Petroleum Congress (1951).
9. Leblanc, J.L. and Caudle, B.H.: "A Streamline Model for Secondary Recovery," *SPEJ* (March 1971), 7-13.
10. Higgins R.V. and Leighton, A.J.: "A Computer Method to Calculate Two-Phase Flow in Any Irregularly Bounded Porous Medium," *JPT* (June 1962) 14, 679-683.
11. Yih, C.: "Stream Functions in Three-Dimensional Flow," *La Houille Blanche* (1957) **3**,445-45
12. Pollock, D.W.: "Semianalytical Computation of Path Lines for Finite-Difference Models," *Ground Water* (November-December 1988) **26**, No. 6, 743-750.

13. Prevost, M., Edwards, M.G., and Blunt, M.J.: "Streamline Tracing on Curvilinear Structured and Unstructured Grids," *SPEJ* (June 2002) 139-148.
14. Cordes, C. and Kinzelbach, W.: "Continuous Groundwater Velocity Fields and Path Lines in Linear, Bilinear and Trilinear Finite Elements," *Water Resources Research* (November 1992) **28**, 11, 2903.
15. Datta-Gupta, A. and King, M.J: "A Semianalytic Approach to Tracer Flow Modeling in Heterogeneous Permeable Media," *Advances in Water Resources* (1995) **18**, 9-24.
16. Bratvedt, F., Gimse, T., Tegnander, C.: "Streamline Computations for Porous Media Flow Including Gravity," *Transport in Porous Media* (October1996) **25**, No.1, 63-78.
17. Rodriguez, P.G., Segura, M.K., and Moreno, F.J.: "Streamline Methodology Using an Efficient Operator Splitting for Accurate Modeling of Capillarity and Gravity Effects," paper SPE 79693 presented at the 2003 Reservoir Simulation Symposium, Houston, TX, 3-5 February.
18. Osako, I., Datta-Gupta, A., and King, M.J.: "Timestep Selection during Streamline Simulation via Transverse Flux Correction," paper SPE 79688 presented at the 2003 Reservoir Simulation Symposium, Houston, TX, 3-5 February.
19. Warren, J.E. and Root, P.J.: "The Behavior of Naturally Fractured Reservoirs", *SPEJ* (September 1963) 245-255; *Trans*., AIME **228**.
20. Kazemi, H. *et al*.: "Numerical Simulation of Water-Oil Flow in Naturally Fractured Reservoirs," *SPEJ* (December 1976) 317-26: *Trans*., AIME **261**.
21. Dean, R.H. and Lo, L.L.: "Simulations of Naturally Fractured Reservoirs," *SPERE* (May 1988) 638-48.
22. Saidi, A.M.: "Simulation of Naturally Fractured Reservoirs," paper SPE 12270 presented at the 1983 SPE Symposium on Reservoir Simulation, San Francisco, California, 15-18 November.
23. Thomas, L. K., Dixon, T.N., and Pierson, R.G.: "Fractured Reservoir Simulation," *SPEJ* (February 1983) 42-54.

24. Sonier, F., Souillard, P., Blaskovich, F.T.: "Numerical Simulation of Naturally Fractured Reservoirs", SPE paper 15627 presented at the 1986 SPE Annual Technical Conference and Exhibition, New Orleans, 5-8 October.
25. Litvak, B.L.: "Simulation and Characterization of Naturally Fractured Reservoirs", Proceedings of the 1985 Reservoir Characterization Technical Conference, Dallas, April 29-May 1.
26. Gilman, J.R.: "An Efficient Finite-Difference Method for Simulation Phase Segregation in Matrix Blocks in Double Porosity Reservoirs," *SPERE* (July 1986) 403-416.
27. Pruess, K. and Narasimhan, T.N.: "A Practical Method for Modeling Fluid and Heat Flow in Fractured Porous Media," *SPEJ* (February 1985) 14-26.
28. Civan, F.: "Waterflooding of Naturally Fractured Reservoirs: An Efficient Simulation Approach," Paper SPE 25449 presented at the 1993 Production Operations Symposium on Improved Recovery, Tulsa, OK, 17-20 April.
29. Civan, F., Wang, W., and Gupta, A.: "Effect of Wettability and Matrix to Fracture Transfer on the Waterflooding in Fractured Reservoirs," paper SPE 52197 presented at the 1999 SPE Mid-Continent Operations Symposium, Oklahoma City, OK, 28-31 March.
30. DeSwaan, A.: "Theory of Waterflooding in Fractured Reservoirs," *SPEJ* (April 1978) 117-122.
31. Gupta, A. and Civan, F.: "An Improved Model for Laboratory Measurement of Matrix to Fracture Transfer Function Parameters in Immiscible Displacement," paper SPE 28929 presented at the 1994 SPE Annual Technical Conference and Exhibition, New Orleans, 25-28 September.
32. Kazemi, H. *et al*.: "Analytical and Numerical Solution of Oil Recovery From Fractured Reservoirs with Empirical Transfer Functions," *SPEJ* (May 1992) 219.
33. Aronofsky, J.S., Masse, L. and Natanson, S.G.: "A Model for the Mechanism of Oil Recovery from the Porous Matrix Due to Water Invasion in Fractured Reservoirs," *Trans*., AIME (1958) **213**, 17-19.

34. Mattax, C.C. and Kyte, J.R.: "Imbibition Oil Recovery from Fracture Water-Drive Reservoirs," *SPEJ* (June 1962) 177-184; *Trans*., AIME **255**.
35. Terez, I.E. and Firoozabadi, A.: "Water Injection in Water-Wet Fractured Porous Media: Experiments and New Model with Modified Buckley-Leverett Theory," *SPEJ* (June 1999) 134-141.
36. Chen, J.: "New Approaches to Dual Porosity Modeling of Waterflooding in Naturally Fractured Reservoirs," PhD Dissertation, University of Texas at Austin, Austin, TX, (1993).
37. Chen, J., Miller, M.A., and Sepehrnoori, K..: "Theoretical Investigation of Countercurrent Imbibition in Fractured Reservoir Matrix Blocks," paper SPE 29141 presented at 1995 SPE Symposium on Reservoir Simulation, San Antonio, TX, 12-15 February.
38. Cil, M., Reis, J. C., Miller, M.A., and Misra, D.: "An Examination of Countercurrent Capillary Imbibition Recovery from Single Matrix Blocks and Recovery Predictions by Analytical Matrix/fracture Transfer Functions," paper SPE 49005 presented at 1998 SPE Annual Technical Conference and Exhibition, New Orleans, LA, 27-30 September.
39. Hayashi, J.A. and Rosales, C.P.: "Visual Investigation of Imbibition Process," paper SPE 23745 presented at the 1992 SPE Latin American Petroleum Engineering Conference, Caracas, Venezuela, 8-11 March.
40. Hernandez, J.C. and Rosales, C.P.: "Imbibition as a Dispersion Process," paper SPE 23748 presented at the 1992 SPE Latin American Petoleum Engineering Conference, Caracas, Venezuela, 8-11 March.
41. Aziz, K. and settari, A.: *Petroleum Reservoir Simulation*, Applied Science Publisher, Essex, U.K. (1979).
42. Dutra, T.V. and Aziz, K.: "A New Double-Porosity Reservoir Model for Oil-Water Flow Problems," *SPERE* (November 1992) 419.
43. Buckley, S.E. and Leverett, M.C.: "Mechanism of Fluid Displacement in Sands," *Trans*., AIME(1941) **249**, 107-116.

44. Coats, K.H.: "Implicit Compositional Simulation of Single-Porosity and Dual-Porosity Reservoirs," paper SPE 18427 presented at the 1989 SPE Symposium on Reservoir Simulation, Houston, 6-8 February.
45. Rossen, R.H. and Shen, E.I.: "Simulation of Gas/Oil Drainage and Water/Oil Imbibitions in Naturally Fractured Reservoirs," paper SPE 16982 presented at the 1987 SPE Annual Technical Conference and Exhibition, Dallas, 27-30 September.
46. Bourbiaux, B. and Kalaydjian, F.: "Experimental Study of Cocurrent and Countercurrent Flow in Natural Porous Media," *SPERE* (August 1990); *Trans*., AIME, 289.
47. Pooladi-Darvish, M. and Firoozabadi, A.: "Cocurrent and Countercurrent Imbibition in a Water-Wet Matrix Block," *SPEJ* (March 2000) 3-11.
48. Shenawi, S.H., Wu, C.H., and Luan, Z.A.: "A New Iterative Mathematical Model for the Analysis of Imbibition Carbonated Waterflood in Naturally Fractured Reservoirs," paper SPE 27717 presented at the 1994 SPE Permian Basin Oil and Gas Recovery Conference, Midland, TX, 16-18 March.
49. Luan, Z.: "Splitting Pseudospectral Algorithm for Parallel Simulation of Naturally Fractured Reservoirs," paper SPE 30723 presented at the 1995 Annual Technical Conference & Exhibition, Dallas, October 22-25.

APPENDIX I

This appendix discusses the development of Eq.2.72.The modified Bessel function, I_0, in Eq.2.72 is an infinite series.

$$I_0(x) = \sum_{n=0}^{\infty} \frac{1}{n!^2}\left(\frac{x}{2}\right)^{2n} \quad \text{.....(AI-1)}$$

Using Eq.AI-1 and separation of variables concept, Eq.72 can be rewritten in the following form:

$$\begin{aligned} &\Psi = \omega e^{-\beta} \sum_{n=0}^{\infty} \frac{\beta^n \omega^n}{n!^2} \int_0^c e^{ax} x^n dx \\ &x = \varepsilon - \tau / H \\ &c = t - \tau / H \\ &a = -\omega \end{aligned} \quad \text{..... (AI-2)}$$

The integral term in Eq.AI-2 has a general from given as,

$$\mathrm{I} = \int_L^K e^{ax} x^n dx \quad \text{.....(AI-3)}$$

This integral can be solved analytical using the concept of integration by parts. The results is a finite series given as,

$$\mathrm{I} = \left[e^{aK} \sum_{m=0}^{n} (-1)^{n-m} \frac{n! K^m}{a^{(n-m+1)} m!} \right] + \left[e^{aL} \sum_{m=0}^{n} (-1)^{n+1} \frac{n! L^m}{a^{(n-m+1)} m!} \right] \quad \text{.....(AI-4)}$$

By combining Eq.AI-4 and Eq.AI-2, we can arrive at Eq.2.72.

VITA

Ahmed Al-Huthali received his B.S. degree in electrical engineering from King Fahd University of Petroleum and Minerals, Saudi Arabia, in December 1998. He worked for Saudi Aramco from December 1998 to August 2001 in the reservoir management department. Then the company sponsored his M.S. study at Texas A&M University, where he received his degree in August 2003.

His current address: 5 Umar Ibn Abdulaziz
Um Al-Arad
Taif
Saudi Arabia